COMPETITION INSTABILITIES OF SPIKE PATTERNS FOR THE 1-D GIERER-MEINHARDT AND SCHNAKENBERG MODELS ARE SUBCRITICAL

THEODORE KOLOKOLNIKOV *, FRÉDÉRIC PAQUIN-LEFEBVRE †, AND MICHAEL J. WARD ‡

Abstract. Spatially localized 1-D spike patterns occur for various two-component reaction-diffusion (RD) systems in the singular limit of a large diffusivity ratio. A competition instability of a steady-state spike pattern is a linear instability that locally preserves the sum of the heights of the spikes. This instability, which results from a zero-eigenvalue crossing of a nonlocal eigenvalue problem at a certain critical value of the inhibitor diffusivity, has been implicated from full PDE numerical simulations of various RD systems of triggering a nonlinear event leading to spike annihilation. As a result, this linear instability is believed to be a key mechanism for initiating a coarsening process of 1-D spike patterns. As an extension of the linear theory, we develop and implement a weakly nonlinear theory to analyze competition instabilities associated with symmetric two-boundary spike equilibria on a finite 1-D domain for the Gierer-Meinhardt and Schnakenberg RD models. Two symmetric boundary spikes interacting through a long-range bulk diffusion field is the simplest spatial configuration of interacting localized spikes that can undergo a competition instability. Within a neighborhood of the parameter value for the competition instability threshold, a multi-scale asymptotic expansion is used to derive an explicit amplitude equation for the heights of the boundary spikes. This amplitude equation confirms that the competition instability is subcritical and, moreover, it shows that the competition instability threshold corresponds to a symmetry-breaking bifurcation point where an unstable branch of asymmetric two-boundary spike equilibria emerges from the symmetric branch. Results from our weakly nonlinear analysis are confirmed from full numerical solutions of the steady-state problem using numerical bifurcation software.

1. Introduction.

Spike patterns are a common class of localized structures that can occur for certain 1-D two-component reaction-diffusion (RD) systems in the singular limit of a large diffusivity ratio. In the large diffusivity ratio, localized spikes in the solution component with small diffusivity interact strongly with each other through the effect of the long-range diffusion of the second solution component. In this so-called semi-strong regime, there is a rather well-developed theory to analyze the existence, linear stability, and slow dynamics of 1-D spike patterns in a variety of specific RD systems such as the Gierer-Meinhardt, Gray-Scott and Brusselator models (see [5], [6], [7], [8], [14], [13], [17], [18], [20], [22], [29], [23], [25], [30] and the references therein). Through linear stability analysis, combined with numerically-generated global bifurcation diagrams and full PDE simulations, it is well-known that spike patterns for certain RD systems can exhibit a variety of instabilities such as, temporal oscillations in the height of the spikes, spike annihilation events, and spike self-replication. In particular, a competition instability is a linear instability of a steady-state spike pattern that locally preserves the sum of the heights of the spikes, and it occurs most typically when the long-range diffusivity exceeds a threshold or when spikes become too-closely spaced (cf. [13], [29], [18], [23]). Based on observations from full PDE numerical simulations of various RD systems, it has been conjectured that this linear instability provides the trigger for the onset of fully nonlinear events leading to the ultimate annihilation of certain spikes in a 1-D spike pattern (cf. [14], [22]). As a result, this instability is believed to be a key mechanism in initiating a coarsening process of 1-D spike patterns. More recently, in [1], spike annihilation events in 1-D have been interpreted in terms of saddle-node points and bifurcations that are associated with quasi-equilibrium manifolds for the heights of the spikes. These manifolds depend on the instantaneous locations of the spikes in the domain and they evolve slowly in time as the spikes drift towards their steady-state spatial configuration.

Motivated by these previous numerical PDE studies exhibiting spike annihilation events, we develop and implement a weakly nonlinear theory to analyze whether competition instabilities of spike patterns for the singularly perturbed 1-D Gierer-Meinhardt and Schnakenberg RD models are subcritical. To facilitate the analysis we will focus only on competition instabilities associated with symmetric two-boundary spike equilibria. For this simple spatial pattern, the linearization of the RD

*Department of Mathematics and Statistics, Dalhousie University, Halifax, Canada. (tkolokol@gmail.com)
†Department of Mathematics, UBC, Vancouver, Canada. (paquinl@math.ubc.ca)
‡Department of Mathematics, UBC, Vancouver, Canada. (corresponding author ward@math.ubc.ca)

system around the steady-state leads to a nonlocal eigenvalue problem (NLEP) whose unstable discrete eigenvalues correspond to an instability in the heights of the two boundary spikes. A competition instability of the spike heights is an instability due to a zero-eigenvalue crossing of the NLEP, and it has the effect of locally preserving the sum of the heights of the two boundary spikes. In contrast to the more delicate case of performing a weakly nonlinear analysis for spike patterns interior to the domain, for boundary-spike patterns there is no complicating feature due to the small eigenvalues in the linearization that are associated with the slow dynamics of the centers of the spikes.

A multi-scale perturbation framework is a well-established theoretical approach for analyzing the weakly nonlinear development of small amplitude patterns near bifurcation points for PDE models, and it has been used in a wide variety of applications (cf. [3], [27]). When the base-state is spatially uniform, it is rather straightforward to derive amplitude, or normal form, equations characterizing the onset and stability of bifurcating small amplitude spatially non-uniform structures that occur near the bifurcation point. In contrast, it is considerably more challenging to implement a weakly nonlinear theory to analyze the branching behavior near bifurcation points associated with localized structures, such as spikes, for singularly perturbed RD systems. In this spatially non-uniform context, there are several key challenges in implementing a weakly nonlinear theory based on multi-scale perturbation theory. The first challenge is that the linearization of the RD system around a localized spike solution leads to a singularly perturbed eigenvalue problem in which the underlying linearized operator has spatially variable coefficients. As such, a singular perturbation approach for this eigenvalue problem is needed to identify bifurcation points and to formulate a solvability condition based on the adjoint spectral problem, which is required to derive the amplitude equation. The second key challenge is that certain spatially inhomogeneous boundary value problems (BVPs) arise at various orders in the multi-scale expansion and, most typically, these problems can only be solved numerically. For singularly perturbed reaction-diffusion systems in the weak-interaction regime, characterized by an exponentially weak inter-spike interaction, a weakly nonlinear theory based on center-manifold and multi-scale perturbation theory has been used previously (cf. [9], [2]) to analyze typical spike-drift instabilities, such as spike-layer oscillations and spike pinning, for a wide range of applications.

In contrast, there have only been a few previous weakly nonlinear analyses of localized spike patterns near bifurcation points for singularly perturbed RD systems in which the localized spikes interact strongly through a long-range bulk diffusion field (the so-called semi-strong regime). For such a 1-D spike steady-state solution, a weakly nonlinear analysis of a temporal oscillation in the height of the spike, referred to as a breathing instability and resulting from a Hopf bifurcation of the linearization, was developed recently for the Schnakenberg model and the GM model and its variants in [26], [11] and [12]. For these RD models, an amplitude equation characterizing the local branching behavior of breathing oscillations was derived in terms of coefficients that must be computed numerically from some BVPs. This hybrid analytical-numerical approach showed that, in certain parameter regimes, the Hopf bifurcation for temporal spike height oscillations is subcritical. This theoretical result supports numerical evidence, based on full PDE simulations that small amplitude temporal oscillations of a spike can be unstable in certain parameter regimes, and can trigger a fully nonlinear event leading to the oscillatory collapse of a spike. In a 2-D spatial context, a weakly nonlinear analysis was recently undertaken in [32] to show that a small amplitude peanut-shaped instability of a locally radially symmetric spot solution to the singularly perturbed Schnakenberg and Brusselator RD models is always subcritical. This theoretical result provides a partial explanation for observations based on numerical PDE simulations of these RD models that, near a critical value of the feed-rate, a non-radially symmetric peanut-shape deformation of a localized spot can trigger a fully nonlinear spot self-replication event (see [32] and [27] for references in this area).

Our analysis will focus on two-boundary spike equilibria for the 1-D GM and Schnakenberg RD models in the semi-strong spike interaction regime. The dimensionless prototypical GM model [10]

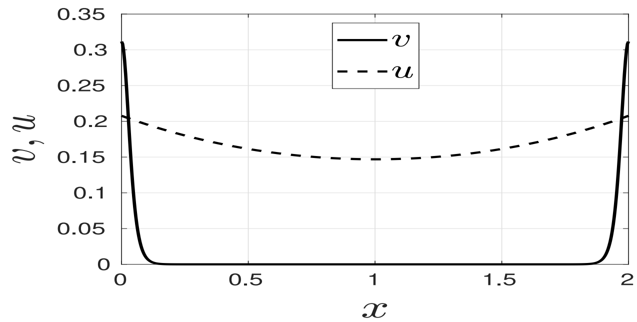

FIG. 1. *Plot of the asymptotic result for the steady-state two-boundary spike solution for the GM model* (1.1) *when* $L = 2$*,* $\varepsilon = 0.02$*, and* $\mu = 0.7768$*. The inhibitor* u *is given by* (2.5) *while the activator* v *is* $v \sim U_0 \left[w\left(\varepsilon^{-1}x\right) + w\left(\varepsilon^{-1}(L-x)\right)\right]$*, where* $w(y)$ *is the homoclinic in* (2.3) *and* U_0 *is given in* (2.5)*.*

for the activator v and inhibitor u on the 1-D domain $0 \leq x \leq L$ is conveniently formulated as

$$v_t = \varepsilon^2 v_{xx} - v + \frac{v^2}{u}\,, \qquad \tau_0 u_t = u_{xx} - \mu u + \varepsilon^{-1} v^2\,, \tag{1.1}$$

with $v_x = u_x = 0$ at $x = 0, L$. Here $\varepsilon \ll 1$, $\mu = \mathcal{O}(1)$ and $\tau_0 = \mathcal{O}(1)$ are positive constants. In this non-dimensionalization of the GM model, where the inhibitor diffusivity is set to unity, the key bifurcation parameter μ represents the decay rate for the inhibitor in the bulk region $0 < x < L$. As μ decreases, the interaction of the spatially segregated boundary spikes near $x = 0$ and $x = L$ increases, until eventually a competition instability occurs at some critical value $\mu = \mu_c$. For μ below this critical value, symmetric two-boundary spike equilibria are unstable. In Fig. 1 we plot the steady-state symmetric two-boundary spike solution for $L = 2$, $\mu = \mu_c \approx 0.7768$, and $\varepsilon = 0.02$. For $L = 2$ and $\varepsilon = 0.02$, in the left panel of Fig. 2 we plot time-dependent PDE results for (1.1) for the amplitudes $v(0, t)$ and $v(L, t)$ of the two boundary spikes, which shows that a competition instability in the spike amplitudes occurs as μ is slowly ramped in time below the competition instability threshold μ_c. This instability is observed to trigger a fully nonlinear boundary spike annihilation event. In terms of the maximum $\max(u(0, t), u(L, t))$ of the inhibitor field, in the right panel of Fig. 2 we superimpose these results from the PDE simulation on the global bifurcation diagram of two- and one-boundary spike equilibria for (1.1). This figure shows that the slow ramping in μ below the competition instability threshold triggers a transition between a symmetric two-boundary spike steady-state and a one-boundary spike steady-state. At the competition instability threshold value of μ, we observe that an unstable (subcritical) asymmetric branch of two-boundary spike equilibria emerges. One main goal of this paper is to provide a detailed analysis of this local branching behavior. From the left panel of Fig. 2, we observe that although the linear competition instability initially preserves the sum of the spike amplitudes, this conservation principle does not hold at later times. We remark that although the time-dependent ramping of μ provides the simplest numerical approach for illustrating the onset of the competition instability and the ultimate long-time fate of the two-boundary spike pattern, one must expect a delayed onset of the instability that is independent of the speed of ramping, as is typical in transcritical or pitchfork bifurcation problems in simple ODE systems (cf. [19]). This delayed onset is evident in both panels of Fig. 2. Delayed competition instabilities and delayed Hopf bifurcations for spike patterns due to slow parameter ramping have been analyzed in [24] for a few RD systems (see also [15] and the references therein).

Similarly, the dimensionless Schnakenberg model on the 1-D domain $0 \leq x \leq L$ is formulated as

$$v_t = \varepsilon^2 v_{xx} - v + uv^2\,, \qquad \tau_0 u_t = u_{xx} + \mu - \varepsilon^{-1} uv^2\,, \tag{1.2}$$

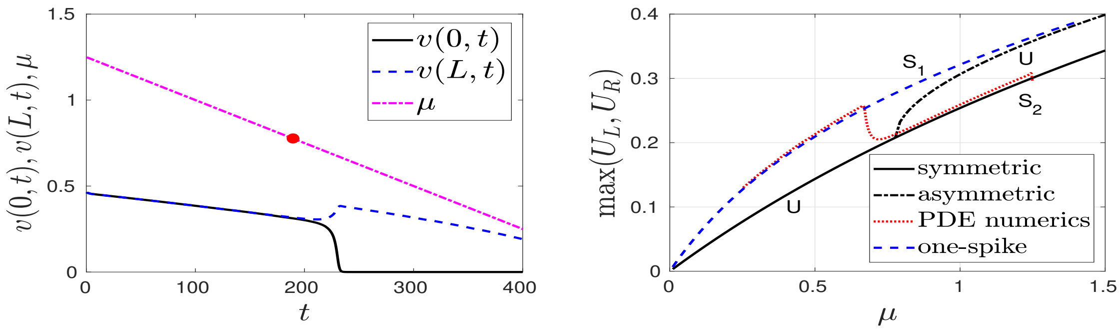

FIG. 2. *Left panel: Plot of the spike heights $v(0,t)$ and $v(L,t)$ versus time, as computed from (1.1), showing a competition instability followed by a boundary spike annihilation event as μ is ramped below $\mu_c \approx 0.7768$ (red dot) with $\mu = 1.25 - \delta t$ and $\delta = 0.0025$. Since the slow ramping in μ induces the typical delayed bifurcation effect, the onset of the instability occurs for $\mu < \mu_c$. Parameters in (1.1) are $L = 2$, $\varepsilon = 0.02$, and $\tau_0 = 0.2$. Right panel: Plot of* $\max(U_L, U_R)$, *where $U_L \equiv u(0)$ and $U_R \equiv u(L)$, for the inhibitor field versus μ for the global branches of symmetric (black solid curve) and asymmetric (black dashed-dotted curve) two-boundary spike equilibria and a one-boundary spike (blue dashed curve) equilibrium. The labeled linear stability properties are as follows: U: linearly unstable for all $\tau_0 > 0$. S_1: a one-boundary spike steady-state is linearly stable if $0 \leq \tau_0 < \tau_{H1}(\mu)$ (see Fig. 3). S_2: a symmetric two-boundary spike steady-state is linearly stable if $0 \leq \tau_0 < \min(\tau_{H+}(\mu), \tau_{H-}(\mu))$ (see Fig. 3). The dotted red curve is from the time-dependent PDE simulation of (1.1) shown in the left panel. The slow ramping of μ below the competition instability threshold at $\mu = \mu_c \approx 0.7768$ is observed to trigger a (delayed) transition to a one-boundary spike solution.*

with $v_x = u_x = 0$ at $x = 0, L$. Here $\varepsilon \ll 1$, $\mu = \mathcal{O}(1)$ and $\tau_0 = \mathcal{O}(1)$ are positive constants. In this context, the bifurcation parameter μ is the feed-rate or "fuel" from the external substrate. As μ is decreased below some threshold μ_c, there is insufficient "fuel" to support a stable symmetric two-boundary spike steady-state, and this solution is destabilized through a competition instability. We remark that our weakly nonlinear approach for analyzing competition instabilities for (1.1) and (1.2) shares some similarities with the theoretical framework developed in [21] for analyzing instabilities associated with dynamically active 1-D membranes that are coupled via a passive bulk diffusion field.

The outline of this paper is as follows. For the GM model (1.1), in §2 a symmetric two-boundary spike steady-state is constructed using matched asymptotic expansions for $\varepsilon \ll 1$. In §2.1 we derive and analyze an NLEP whose spectrum characterizes the linear stability of this steady-state. From this NLEP we derive the critical value μ_c of μ, given in (2.17), at which the symmetric two-boundary spike loses stability to an anti-phase perturbation of the heights of the two boundary spikes. This competition instability results from a zero-eigenvalue crossing of the NLEP, and when τ_0 is below a Hopf bifurcation threshold there are no additional unstable discrete eigenvalues of the NLEP. In §3 we formulate and implement a weakly nonlinear analysis to derive an amplitude equation characterizing the branching behavior associated with the competition instability when $\mu - \mu_c = \mathcal{O}(\sigma^2)$. By using a boundary-layer theory for $\varepsilon \ll 1$ to calculate the terms at various orders in σ in the multi-scale expansion, we obtain explicit analytical results for the coefficients in the amplitude equation when $\varepsilon \ll 1$. This amplitude equation confirms that the competition instability is in fact subcritical. From an asymptotic construction of asymmetric two-boundary spike equilibria in §3.2 for $\varepsilon \ll 1$, we show explicitly that the competition instability threshold corresponds to a symmetry-breaking bifurcation point where an unstable branch of asymmetric two-boundary spike equilibria emerges from the symmetric solution branch. Moreover, in terms of the bifurcation parameter μ, we confirm our weakly nonlinear analysis with corresponding numerical results computed using the bifurcation software COCO [4] after first spatially discretizing the BVP system for the steady-state of the GM model (1.1) when $\varepsilon = 0.01$.

For the Schnakenberg model (1.2), in §4 we perform a similar weakly nonlinear analysis near the bifurcation point $\mu = \mu_c$ to establish that competition instabilities for symmetric two-boundary spike steady-states are also subcritical. In §4.3 we show that, as similar to that for the GM model, the competition instability threshold corresponds to a symmetric-breaking bifurcation point at which an unstable branch of asymmetric two-boundary spike equilibria emerge from the symmetric branch.

In §5 we construct solution branches of asymmetric and symmetric two-boundary spike equilbria for an extended GM model with a general exponent set for the nonlinear reaction kinetics. The branching structure associated with this steady-state analysis suggests that competition instabilities for this generalized GM model are also subcritical. The paper concludes with a brief discussion in §6.

2. Gierer-Meinhardt Model. We use the method of matched asymptotic expansions to construct a symmetric steady-state boundary spike solution to (1.1) with spikes at $x = 0$ and $x = L$. We only focus on the boundary layer near $x = 0$ since we can impose the symmetry condition $u_x = v_x = 0$ at the midpoint $x = L/2$.

In the boundary layer region near $x = 0$, we let $U(y) = u(\varepsilon y)$ and $V(y) = v(\varepsilon y)$ and we expand

$$V = V_0(y) + \varepsilon V_1(y) + \dots , \qquad U = U_0(y) + \varepsilon U_1(y) + \dots , \quad \text{with} \quad y = \varepsilon^{-1} x . \tag{2.1}$$

Upon substituting (2.1) into the steady-state problem for (1.1), and collecting powers of ε, we obtain that U_0 is a constant to be determined, and that

$$V_{0yy} - V_0 + \frac{V_0^2}{U_0} = 0 , \qquad U_{1yy} = -V_0^2 , \qquad y \geq 0 , \tag{2.2}$$

with $V_{0y} = U_{1y} = 0$ at $y = 0$. We conclude that $V_0 = U_0 w(y)$, where

$$w = \frac{3}{2} \mathrm{sech}^2 \left(y/2 \right) , \tag{2.3}$$

is the homoclinic solution to $w_{yy} - w + w^2 = 0$ on $y \geq 0$. From integrating the U_1 equation in (2.2), we get the far-field behavior $U_y \sim \varepsilon U_{1y} = -\varepsilon U_0^2 \int_0^\infty w^2 \, dy$ as $y \to +\infty$. This expression provides the matching condition for the outer solution for the inhibitor u as $x \to 0^+$.

In the outer region, v is exponentially small while from the steady-state of (1.1), and from matching to the boundary layer solution, we obtain that u satisfies

$$u_{xx} - \mu u = 0 , \quad 0 \leq x \leq L/2 ; \qquad u_x(0^+) = -U_0^2 \left(\int_0^\infty w^2 \, dy \right) , \quad u_x \left(L/2 \right) = 0 , \tag{2.4}$$

with $u(0^+) = U_0$. The solution to (2.4) on $0 < x \leq L/2$ is

$$u(x) = U_0 \frac{\cosh \left[\sqrt{\mu} \left(x - L/2 \right) \right]}{\cosh \left[\sqrt{\mu} L/2 \right]} , \qquad U_0 = \frac{\sqrt{\mu}}{b} \tanh \left(\frac{\sqrt{\mu} L}{2} \right) , \qquad b \equiv \int_0^\infty w^2 \, dy . \tag{2.5}$$

The solution on $L/2 \leq x < L$ is obtained from an even extension about $x = L/2$.

2.1. Linear Stability Analysis. To formulate the linear stability problem, we let v_e and u_e denote the steady-state solution for (1.1) and we substitute $v = v_e + e^{\lambda t} \phi(x)$ and $u = u_e + e^{\lambda t} \eta(x)$ into (1.1) and linearize. This yields the following eigenvalue problem on $0 \leq x \leq L$:

$$\varepsilon^2 \phi_{xx} - \phi + \frac{2 v_e}{u_e} \phi - \frac{v_e^2}{u_e^2} \eta = \lambda \phi ; \qquad \phi_x = 0 \quad \text{at} \ \ x = 0, L , \tag{2.6a}$$

$$\eta_{xx} - \left(\mu + \tau_0 \lambda \right) \eta = -2 \varepsilon^{-1} v_e \phi ; \qquad \eta_x = 0 \quad \text{at} \ \ x = 0, L . \tag{2.6b}$$

Since the spikes are centered at $x = 0$ and $x = L$, we look for a localized eigenfunction for (2.6a) in terms of some constants c_1 and c_2 in the form

$$\phi(x) = c_1 \Phi(x/\varepsilon) + c_2 \Phi \left[(L - x)/\varepsilon \right] . \tag{2.7}$$

Since $v_e/u_e \sim w$ near each endpoint, we obtain from (2.6a) that $\Phi(y)$ satisfies

$$c_j L_0 \Phi - w^2 \eta(x_j) = \lambda c_j \Phi\,, \qquad 0 \le y < \infty\,, \qquad \text{where} \qquad L_0\Phi \equiv \Phi_{yy} - \Phi + 2w\Phi\,. \tag{2.8}$$

Here $\eta(x_1)$ and $\eta(x_2)$ are the constant leading-order approximations for $\eta(x)$ near $x_1 \equiv 0$ and $x_2 \equiv L$, which are to be determined by matching the boundary layer regions to an outer expansion.

In the inner region near $x = 0$ we expand $\eta = \eta(x_1) + \varepsilon \eta_1(y) + \ldots$, with $y = x/\varepsilon$, to obtain, upon collecting $\mathcal{O}(\varepsilon^{-1})$ terms in (2.6b), that

$$\eta_{1yy} = -2c_1 U_0 w\,\Phi\,, \quad 0 \le y < \infty\,; \qquad \eta_{1y}(0) = 0\,, \tag{2.9}$$

so that $\lim_{y\to\infty} \eta_{1y} = -2c_1 U_0 \int_0^\infty w\Phi\, dy$. This provides the matching condition for the leading-order outer solution, denoted by $N_0(x)$, in the form $N_{0x} \to \lim_{y\to\infty} \eta_{1y}$ and $N_0 \to \eta(0)$ as $x \to 0^+$. In a similar way near $x = L$, we set $y = (L-x)/\varepsilon$ and we expand $\eta = \eta(x_2) + \varepsilon\eta_1(y) + \ldots$, to obtain

$$\eta_{1yy} = -2c_2 U_0 w\Phi\,, \quad 0 \le y < \infty\,; \qquad \eta_{1y}(0) = 0\,, \tag{2.10}$$

which yields $\lim_{y\to\infty} \eta_{1y} = -2c_2 U_0 \int_0^\infty w\Phi\, dy$ and the matching conditions $N_{0x} \to -\lim_{y\to\infty}\eta_{1y}$ and $N_0 \to \eta(L)$ as $x \to L^-$ for the outer solution. By using these matching conditions we conclude that the leading-order outer solution $N_0(x)$ for (2.6b) satisfies

$$\begin{aligned} &N_{0xx} - (\mu + \tau_0\lambda)\, N_0 = 0\,, \quad 0 < x < L\,; \qquad N_0(0) = \eta(0^+)\,, \quad N_0(L^-) = \eta(L)\,, \\ &N_{0x}(0^+) = -2c_1 U_0 \int_0^\infty w\Phi\, dy\,, \qquad N_{0x}(L^-) = 2c_2 U_0 \int_0^\infty w\Phi\, dy\,. \end{aligned} \tag{2.11}$$

The solution to (2.11) is

$$N_0(x) = N_{0x}(L^-) \frac{\cosh(\theta_\lambda x)}{\theta_\lambda \sinh(\theta_\lambda L)} - N_{0x}(0^+) \frac{\cosh(\theta_\lambda (L-x))}{\theta_\lambda \sinh(\theta_\lambda L)}\,, \qquad \theta_\lambda \equiv \sqrt{\mu + \tau_0 \lambda}\,, \tag{2.12}$$

where we have specified the principal branch for the square root for θ_λ. We then set $N(0^+) = \eta(0)$ and $N(L^-) = \eta(L)$, and use (2.5) for U_0. This yields that

$$\begin{pmatrix} \eta(0) \\ \eta(L) \end{pmatrix} = \frac{2\sqrt{\mu}}{\sqrt{\mu + \tau_0\lambda}} \tanh\left(\frac{\sqrt{\mu}L}{2}\right) (\mathcal{G}_\lambda \mathbf{c}) \left(\frac{\int_0^\infty w\Phi\, dy}{\int_0^\infty w^2\, dy} \right)\,, \tag{2.13a}$$

where the 2×2 symmetric and cyclic Green's matrix $\mathcal{G}_\lambda$ and $\mathbf{c}$ are given by

$$\mathcal{G}_\lambda \equiv \begin{pmatrix} \coth(\theta_\lambda L) & \operatorname{csch}(\theta_\lambda L) \\ \operatorname{csch}(\theta_\lambda L) & \coth(\theta_\lambda L) \end{pmatrix}\,, \qquad \mathbf{c} \equiv \begin{pmatrix} c_1 \\ c_2 \end{pmatrix}\,. \tag{2.13b}$$

Upon substituting (2.13) into (2.8), we obtain the vector-valued NLEP

$$(L_0\Phi)\,\mathbf{c} - \frac{2w^2\sqrt{\mu}}{\sqrt{\mu+\tau_0\lambda}} \tanh\left(\frac{\sqrt{\mu}L}{2}\right) (\mathcal{G}_\lambda \mathbf{c}) \left(\frac{\int_0^\infty w\Phi\, dy}{\int_0^\infty w^2\, dy} \right) = \lambda \Phi \mathbf{c}\,. \tag{2.14}$$

Since $\mathcal{G}_\lambda$ is symmetric and cyclic, its matrix spectrum $\mathcal{G}_\lambda \mathbf{c} = \kappa \mathbf{c}$ is readily calculated as

$$\begin{aligned} &\mathbf{c}_+ \equiv \begin{pmatrix} 1 \\ 1 \end{pmatrix}\,, \quad \text{in-phase } (+)\,; \quad \kappa_+ \equiv \coth(\theta_\lambda L) + \operatorname{csch}(\theta_\lambda L) = \coth\left(\frac{\theta_\lambda L}{2}\right)\,, \\ &\mathbf{c}_- \equiv \begin{pmatrix} 1 \\ -1 \end{pmatrix}\,, \quad \text{anti-phase } (-)\,; \quad \kappa_- \equiv \coth(\theta_\lambda L) - \operatorname{csch}(\theta_\lambda L) = \tanh\left(\frac{\theta_\lambda L}{2}\right)\,. \end{aligned} \tag{2.15}$$

Defining $\mathcal{Q} \equiv (\mathbf{c}_+, \mathbf{c}_-)$, $\Lambda = \mathrm{diag}(\kappa_+, \kappa_-)$ and $\mathbf{b} \equiv \mathcal{Q}^{-1}\mathbf{c}$, we use $\mathcal{G}_\lambda = \mathcal{Q}\Lambda\mathcal{Q}^{-1}$ to obtain that (2.14) reduces to the following scalar NLEPs, defined on $0 \le y < \infty$, governing the linear stability of the steady-state two-boundary spike solution to either in-phase (+) or anti-phase (−) perturbations:

$$L_0\Phi - \chi_\pm(\lambda,\mu) w^2 \left(\frac{\int_0^\infty w\Phi\, dy}{\int_0^\infty w^2\, dy} \right) = \lambda\Phi \,; \qquad \Phi_y(0) = 0 \,, \quad \lim_{y\to\infty} \Phi(y) = 0 \,. \tag{2.16a}$$

In (2.16a) the two choices for the multiplier $\chi_\pm(\lambda,\mu)$ of the NLEP are

(2.16b)

$$\chi_+(\lambda,\mu) = \frac{2\sqrt{\mu}}{\sqrt{\mu+\tau_0\lambda}} \frac{\tanh\left(\sqrt{\mu}L/2\right)}{\tanh\left(\theta_\lambda L/2\right)} \,, \qquad \chi_-(\lambda,\mu) = \frac{2\sqrt{\mu}}{\sqrt{\mu+\tau_0\lambda}} \frac{\tanh\left(\sqrt{\mu}L/2\right)}{\coth\left(\theta_\lambda L/2\right)} \,; \quad \theta_\lambda \equiv \sqrt{\mu+\tau_0\lambda} \,.$$

Since NLEPs of the general form (2.16) have been analyzed previously in [29] and [22], we now only briefly summarize the main results for the spectrum of (2.16).

For the in-phase mode, we have spectral stability, i.e. $\mathrm{Re}(\lambda) < 0$, only when $\tau_0 < \tau_{H+}(\mu)$. Here $\tau_{H+}(\mu)$ is a Hopf bifurcation threshold, depending on μ, for the in-phase mode for which $\lambda = \pm i\lambda_{IH+}(\mu)$ is an eigenvalue for (2.16). In contrast, for the anti-phase mode, we have an unstable real positive eigenvalue of the NLEP for any $\tau_0 \ge 0$ whenever $\mu < \mu_c$, where μ_c satisfies

$$\sinh\left(\sqrt{\mu_c}L/2\right) = 1 \qquad \text{so that} \qquad \mu_c \equiv \frac{4}{L^2}\left[\ln(1+\sqrt{2})\right]^2 \,. \tag{2.17}$$

This critical value of μ, termed the competition instability threshold, is characterized by

$$\chi_-(0,\mu) = 1 \,, \qquad \lambda = 0 \,, \qquad \Phi = w \,, \tag{2.18}$$

which follows by using the identity $L_0 w = w^2$ together with the explicit expression for χ_- given in (2.16b). On the range $\mu > \mu_c$, there is additionally a Hopf bifurcation that occurs when $\tau = \tau_{H-}(\mu)$ and $\lambda = \pm i\lambda_{IH-}(\mu)$. As $\mu \to \mu_c$ from above, we have that $\lambda_{IH-}(\mu) \to 0$. For $L = 2$, in Fig. 3 we illustrate these linear stability results for both the in-phase and anti-phase modes in the τ_0 versus μ parameter plane. In particular, for $L = 2$ and $\mu = \mu_c \approx 0.7768$ we calculate that

$$\tau_{H+} \approx 0.9336 \,, \qquad \tau_{H-} = \frac{3\sqrt{2}\mu_c}{2}\left[\sqrt{2} - \ln(1+\sqrt{2})\right]^{-1} \approx 3.981\mu_c \approx 3.0925 \,. \tag{2.19}$$

In Appendix A we give the procedure, similar to that of [22], for numerically computing the Hopf bifurcation curves shown in Fig. 3. Moreover, we derive the explicit result in (2.19) for τ_{H-} at $\mu = \mu_c$. In Fig. 3 we also give corresponding results for the Hopf bifurcation threshold, τ_{H1}, and pure imaginary eigenvalue λ_{I1} for the linearization of a one-boundary spike steady-state solution. Since the stability threshold for this one-boundary spike solution is equivalent to that for an interior spike solution on a domain of twice the length, we conclude from [29] that the one-boundary spike steady-state is linearly stable for all $\mu > 0$ provided that $\tau_0 < \tau_{H1}(\mu)$.

3. Weakly Nonlinear Analysis.

We now perform a weakly nonlinear analysis near the zero-eigenvalue crossing at $\mu = \mu_c$ for the anti-phase mode when $0 \le \tau_0 < \min(\tau_{H+}(\mu_c), \tau_{H-}(\mu_c)) = \tau_{H+}(\mu_c) \approx 0.9336$. As discussed in §2.1, this zero-eigenvalue crossing corresponds to the onset of the sign-fluctuating competition instability of the two boundary spikes. To perform a weakly nonlinear analysis of this instability, we first introduce a neighborhood near μ_c and a slow time scale T by

$$\mu = \mu_c - k\sigma^2 \,, \qquad k = \pm 1 \,, \qquad \mu_c \equiv \frac{4}{L^2}\left[\ln(1+\sqrt{2})\right]^2 \,; \qquad T = \sigma^2 t \,, \tag{3.1}$$

where $\sigma \ll 1$. On this time-scale, we obtain from (1.1) that $v(x,T)$ and $u(x,T)$ satisfy

$$\sigma^2 v_T = \varepsilon^2 v_{xx} - v + \frac{v^2}{u} \,, \quad \tau_0\sigma^2 u_T = u_{xx} - (\mu_c - k\sigma^2)u + \varepsilon^{-1}v^2 \,; \qquad u_x = v_x = 0 \ \text{ at } x = 0, L \,. \tag{3.2}$$

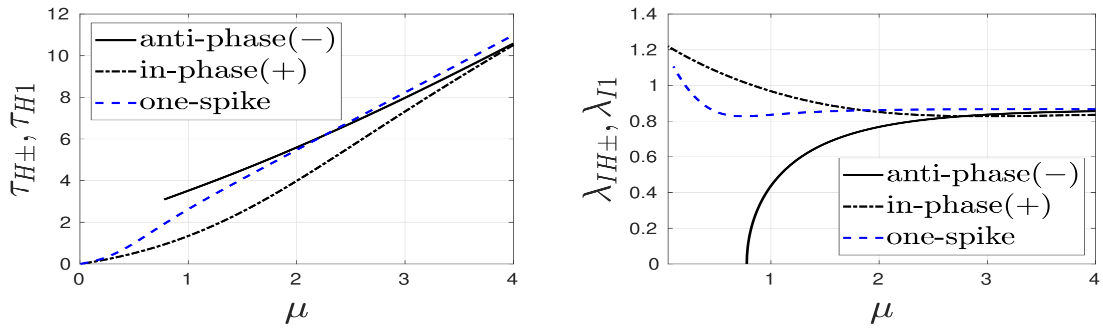

FIG. 3. *Spectral results from NLEP theory for the linearization of symmetric two-boundary spike equilibria for the GM model (1.1). Numerically computed Hopf bifurcation thresholds $\tau_{H\pm}$ (left panel) and corresponding imaginary parts $\lambda_{IH\pm}$ (right panel) of the eigenvalues of the NLEP (2.16) versus μ when $L=2$, as computed using Newton's method on (A.1), for both the in-phase $(+)$ and anti-phase $(-)$ modes. The Hopf threshold for the anti-phase mode exists only when $\mu>\mu_c$, where $\mu_c = 4L^{-2}[\ln(1+\sqrt{2})]^2$. For $L=2$, as μ_c tends to 0.7768 from above we have $\tau_{H-}\approx 3.0925$ and $\lambda_{IH-}\to 0$. At $\mu=\mu_c$, the Hopf threshold for the in-phase mode is $\tau_{H+}\approx 0.9336$. For any $\mu<\mu_c$, the anti-phase mode is always unstable due to a positive real eigenvalue for the NLEP (2.16). For $\mu>\mu_c$, the two-boundary spike solution is linearly stable only when $\tau_0<\min(\tau_{H-},\tau_H+)$. The dashed blue curves are the corresponding results τ_{H1} and λ_{I1} for a one-boundary spike steady-state solution.*

We let $v_e(x)$ and $u_e(x)$ denote the steady-state two-boundary spike solution and we expand

$$
\begin{aligned}
v &= v_e(x) + \sigma v_1(x,T) + \sigma^2 v_2(x,T) + \sigma^3 v_3(x,T) + \dots\,, \\
u &= u_e(x) + \sigma u_1(x,T) + \sigma^2 u_2(x,T) + \sigma^3 u_3(x,T) + \dots\,,
\end{aligned}
\tag{3.3}
$$

where v_e, u_e, v_j and u_j for $j=1,\dots,3$ can depend on ϵ. In our expansion, we will treat ϵ and σ as independent parameters. Upon substituting (3.3) into (3.2), and collecting powers of σ, we obtain the leading order problem on $0\le x\le L$

$$
\varepsilon^2 v_{exx} - v_e + \frac{v_e^2}{u_e} = 0\,, \qquad u_{exx} - \mu_c u_e = -\varepsilon^{-1} v_e^2\,,
\tag{3.4}
$$

and the problem at order $\mathcal{O}(\sigma)$:

$$
\varepsilon^2 v_{1xx} - v_1 + \frac{2v_e}{u_e} v_1 = \frac{v_e^2}{u_e^2} u_1\,, \qquad u_{1xx} - \mu_c u_1 = -2\varepsilon^{-1} v_e v_1\,.
\tag{3.5}
$$

From the $\mathcal{O}(\sigma^2)$ terms we obtain that

$$
\begin{aligned}
\varepsilon^2 v_{2xx} - v_2 + \frac{2v_e}{u_e} v_2 &= \frac{v_e^2}{u_e^2} u_2 - \frac{v_1^2}{u_e} - \frac{v_e^2}{u_e^3} u_1^2 + \frac{2v_e}{u_e^2} u_1 v_1\,, \\
u_{2xx} - \mu_c u_2 &= -k u_e - \varepsilon^{-1}\left(2 v_e v_2 + v_1^2\right)\,.
\end{aligned}
\tag{3.6}
$$

Finally, after some lengthy but straightforward algebra, the problem at $\mathcal{O}(\sigma^3)$ is

$$
\begin{aligned}
\varepsilon^2 v_{3xx} - v_3 + \frac{2v_e}{u_e} v_3 &= \frac{v_e^2}{u_e^2} u_3 - \frac{2 v_1 v_2}{u_e} + \frac{2v_e}{u_e^2}\left(v_1 u_2 + u_1 v_2\right) - \frac{2v_e^2}{u_e^3} u_1 u_2 \\
&\quad + \frac{v_1^2 u_1}{u_e^2} - \frac{2v_e}{u_e^3} v_1 u_1^2 + \frac{v_e^2}{u_e^4} u_1^3 + v_{1T}\,, \\
u_{3xx} - \mu_c u_3 &= -k u_1 + \tau_0 u_{1T} - \varepsilon^{-1}\left(2 v_e v_3 + 2 v_1 v_2\right)\,.
\end{aligned}
\tag{3.7}
$$

For (3.4)–(3.7) we impose $v_{ex} = u_{ex} = 0$ at $x = 0, L$ and $v_{jx} = u_{jx} = 0$ at $x = 0, L$, for $j = 1, \ldots, 3$.

Although the BVPs (3.4)–(3.7) can be solved numerically for a given ε small but fixed, in order to obtain an explicit analytical theory we will solve (3.4)–(3.7) using a boundary layer theory for $\varepsilon \ll 1$. The key observation is that each v_j is non-negligible only in the boundary layer regions near $x = 0, L$. In these boundary layers, the leading-order-in-ε theory shows that we can approximate u_e and u_j for $j = 1, \ldots, 3$ by pointwise values.

In the boundary layer near $x = 0$ or $x = L$ we have $v_e \sim U_0 w$ and $u_e \sim U_0$, where U_0 is defined in (2.5) and $w(y)$ is the homoclinic given in (2.3) with either $y = x/\varepsilon$ or $y = (L - x)/\varepsilon$. In either boundary layer we obtain from (3.5) that the boundary-layer variables $V_1(y)$ and $U_1(y)$ satisfy

$$L_0 V_1 \equiv V_{1yy} - V_1 + 2wV_1 = w^2 U_1 \,, \qquad U_{1yy} = -2\varepsilon U_0 w V_1 + \mathcal{O}(\varepsilon^2) \,, \tag{3.8}$$

so that to leading-order U_1 is a constant. As shown in §2.1 a competition instability is due to a sign fluctuation in the spike heights in the two boundary layer regions. Since $L_0 w = w^2$, we conclude that

$$\begin{aligned} &U_1 = A(T) + \mathcal{O}(\varepsilon) \,, \quad V_1 = wA(T) + \mathcal{O}(\varepsilon) \,, \quad \text{near } \ x = 0 \,; \\ &U_1 = -A(T) + \mathcal{O}(\varepsilon) \,, \quad V_1 = -wA(T) + \mathcal{O}(\varepsilon) \,, \quad \text{near } \ x = L \,. \end{aligned} \tag{3.9}$$

Our goal is to derive an ODE for $A(T)$, which characterizes the height of the boundary spikes near the competition instability threshold. By integrating the U_1 equation in (3.8), we obtain the following matching conditions between the outer inhibitor field u_1 and the two boundary layer solutions:

$$\begin{aligned} u_1(0^+) = A \,, \quad u_{1x}(0^+) &= \lim_{y\to\infty} \varepsilon^{-1} U_{1y} = -2U_0 \int_0^\infty w V_1 \, dy = -2AU_0 \int_0^\infty w^2 \, dy \,, \\ u_1(L^-) = -A \,, \quad u_{1x}(L^-) &= -\lim_{y\to\infty} \varepsilon^{-1} U_{1y} = 2U_0 \int_0^\infty w V_1 \, dy = -2AU_0 \int_0^\infty w^2 \, dy \,. \end{aligned} \tag{3.10}$$

In this way, we obtain from (3.5) and (3.10) that the outer solution u_1 satisfies

$$\begin{aligned} &u_{1xx} - \mu_c u_1 = 0 \,, \quad 0 < x < L \,; \qquad u_1(0^+) = A \,, \quad u_1(L^-) = -A \,, \\ &u_{1x}(0^+) = -2AU_0 b \,, \quad u_{1x}(L^-) = -2AU_0 b \,; \qquad b \equiv \int_0^\infty w^2 \, dy \,. \end{aligned} \tag{3.11}$$

The solution to (3.11) is

$$u_1(x) = -\frac{2AU_0 b}{\sqrt{\mu}_c \sinh(\sqrt{\mu_c} L)} \left[\cosh(\sqrt{\mu_c} x) - \cosh(\sqrt{\mu_c}(L - x)) \right] .$$

To calculate the pre-factor in $u_1(x)$ we use $U_0 b = \sqrt{\mu_c} \tanh\left(\sqrt{\mu_c} L/2\right)$ as given in (2.5) when $\mu = \mu_c$ together with the identity $2\tanh(z/2)/\sinh(z) = \text{sech}^2(z/2)$ and the fact that $\cosh\left(\sqrt{\mu_c} L/2\right) = \sqrt{2}$, as obtained by using (3.1) for μ_c. This yields that

$$u_1(x) = -\frac{A}{2} \left[\cosh(\sqrt{\mu_c} x) - \cosh(\sqrt{\mu_c}(L - x)) \right] . \tag{3.12}$$

By using the expression for μ_c in (3.1) it is readily verified that $u_1(0) = A$ and $u_1(L) = -A$.

Next, we proceed to analyze the $\mathcal{O}(\sigma^2)$ system in (3.6). We denote $V_{2L}(y)$, with $y = x/\varepsilon$, and $V_{2R}(y)$, with $y = (L - x)/\varepsilon$, to be the inner solutions for v_2 in the left and right boundary layers, respectively. By using $V_1 \sim wA$ and $U_1 \sim A$ in the left layer and $V_1 \sim -wA$ and $U_1 \sim -A$ in the right layer, as given in (3.9), respectively, we readily calculate from (3.6) that

$$\begin{aligned} &L_0 V_{2L} \sim w^2 U_2(0) \,, \qquad U_{2yy} = -\varepsilon(2wU_0 V_{2L} + A^2 w^2) + \mathcal{O}(\varepsilon^2) \,, \qquad \text{(left layer)} \,, \\ &L_0 V_{2R} \sim w^2 U_2(L) \,, \qquad U_{2yy} = -\varepsilon(2wU_0 V_{2R} + A^2 w^2) + \mathcal{O}(\varepsilon^2) \,, \qquad \text{(right layer)} \,. \end{aligned} \tag{3.13}$$

Since $L_0 w = w^2$, we conclude that

$$V_{2L}(y) = U_2(0)w(y)\,, \qquad V_{2R}(y) = U_2(L)w(y)\,. \tag{3.14}$$

Upon using these results for V_{2L} and V_{2R}, we integrate the two expressions in (3.13) for U_{2yy} on $0 < y < \infty$ to obtain asymptotic matching conditions for $u_{2x}(0^+)$ and $u_{2x}(L^-)$.

In this way, we obtain that the outer correction u_2 in (3.6) satisfies

$$\begin{aligned} u_{2xx} - \mu_c u_2 = -k u_e\,, \qquad 0 < x < L\,; \qquad u_2(0^+) = U_2(0)\,, \quad u_2(L^-) = U_2(L)\,, \\ u_{2x}(0^+) = -\left(2U_0U_2(0) + A^2\right) b\,, \qquad u_{2x}(L^-) = \left(2U_0U_2(L) + A^2\right) b\,, \end{aligned} \tag{3.15}$$

where $b = \int_0^\infty w^2\, dy$. When $\mu = \mu_c$, the leading-order approximation for the steady-state solution $u_e(x)$ on $0 < x < L$:, satisfying (3.4), is

$$u_e(x) = \frac{U_0}{4}\left[\cosh(\sqrt{\mu_c}x) + \cosh(\sqrt{\mu_c}(L-x))\right]\,; \qquad U_0 \equiv \frac{\sqrt{\mu_c}}{b}\tanh\left(\frac{\sqrt{\mu_c}L}{2}\right) = \frac{\sqrt{\mu_c}}{\sqrt{2}b}\,. \tag{3.16}$$

We readily verify that $u_e(0) = u_e(L) = U_0$ by using $\sinh\left(\sqrt{\mu_c}L/2\right) = 1$ from (2.17).

Our goal is to determine the constants $U_2(0)$ and $U_2(L)$, which are needed in the derivation of the amplitude equation. To do so, we calculate $u_2(x)$, satisfying (3.15), by first decomposing it as

$$u_2(x) = u_{2h}(x) + u_{2p}(x)\,, \tag{3.17}$$

where the particular solution $u_{2p}(x)$ for (3.15), which is even about $x = L/2$, is

$$u_{2p}(x) = -\frac{U_0 k}{8\sqrt{\mu_c}}\,(x - L/2)\left[\sinh(\sqrt{\mu_c}x) - \sinh(\sqrt{\mu_c}(L-x))\right]\,. \tag{3.18}$$

Upon formulating the problem for u_{2h}, and using $u_{2p}(0) = u_{2p}(L)$ together with $u_{2px}(0) = -u_{2px}(L)$, we obtain after some algebra that $U_2(0)$ and $U_2(L)$ satisfy the matrix problem

$$\left(I - 2\tanh\left(\frac{\sqrt{\mu_c}L}{2}\right)\mathcal{G}\right)\begin{pmatrix} U_2(0) \\ U_2(L)\end{pmatrix} = \left(u_{2p}(0) + \frac{\left[A^2 b + u_{2px}(0)\right]}{\sqrt{\mu_c}}\coth\left(\frac{\sqrt{\mu_c}L}{2}\right)\right)\mathbf{e}\,, \tag{3.19a}$$

where $\mathbf{e} \equiv (1,1)^T$ and $\mathcal{G}$ is the cyclic Green's matrix

$$\mathcal{G} \equiv \begin{pmatrix} \coth(\sqrt{\mu_c}L) & \operatorname{csch}(\sqrt{\mu_c}L) \\ \operatorname{csch}(\sqrt{\mu_c}L) & \coth(\sqrt{\mu_c}L)\end{pmatrix}\,. \tag{3.19b}$$

Since $\mathcal{G}\mathbf{e} = \coth(\sqrt{\mu_c}L/2)\mathbf{e}$, we obtain from (3.19) that

$$U_2(0) = U_2(L) = -u_{2p}(0) - \left[A^2 b + u_{2px}(0)\right]\frac{\coth\left(\sqrt{\mu_c}L/2\right)}{\sqrt{\mu_c}}\,. \tag{3.20}$$

Then, we use (3.18) together with $\sinh\left(\sqrt{\mu_c}L/2\right) = 1$ to calculate

$$\begin{aligned} u_{2p}(0) &= -\frac{kU_0L}{16\sqrt{\mu_c}}\sinh(\sqrt{\mu_c}L) = -\frac{\sqrt{2}kU_0L}{8\sqrt{\mu_c}}\,, \\ u_{2px}(0) &= \frac{kU_0}{8\sqrt{\mu_c}}\left[\sinh(\sqrt{\mu_c}L) + \frac{\sqrt{\mu_c}L}{2}\left(1 + \cosh(\sqrt{\mu_c}L)\right)\right] = \frac{kU_0}{4\sqrt{\mu_c}}\left(\sqrt{2} + \sqrt{\mu_c}L\right)\,. \end{aligned} \tag{3.21}$$

Finally, upon substituting (3.21) into (3.20), and using $U_0 = \sqrt{\mu_c}/(\sqrt{2}b)$, we obtain that

$$U_2(0) = U_2(L) = -\frac{kL}{8b} - \frac{A^2}{U_0} - \frac{\sqrt{2}k}{4b\sqrt{\mu_c}}\,, \quad \text{where} \quad k = \pm 1\,. \tag{3.22}$$

Next, we consider the $\mathcal{O}(\sigma^3)$ problem, given by (3.7), and formulate a solvability condition to derive the amplitude equation. We label $V_{3L}(y)$, with $y = x/\varepsilon$, and $V_{3R}(y)$, with $y = (L-x)/\varepsilon$, to be the inner solution for v_3 in the left and right boundary layers, respectively. We use $V_1 \sim wA$, $U_1 \sim A$, $V_2 \sim wU_2(0)$ and $U_2 \sim U_2(0)$ in the left layer and $V_1 \sim -wA$, $U_1 \sim -A$, $V_2 \sim wU_2(L)$ and $U_2 \sim U_2(L)$ in the right layer, where $U_2(0) = U_2(L)$ as given in (3.22). Upon substituting these expressions into (3.7) we obtain that many terms cancel, leaving only

$$L_0 \begin{pmatrix} V_{3L} \\ V_{3R} \end{pmatrix} - w^2 \begin{pmatrix} U_3(0) \\ U_3(L) \end{pmatrix} = wA' \begin{pmatrix} 1 \\ -1 \end{pmatrix}, \tag{3.23}$$

where $A' = dA/dT$. Moreover, from the u_3 equation in (3.7) we get that

(3.24)
$$U_{3yy} \sim -\varepsilon(2wU_0V_{3L} + 2Aw^2U_2(0))\,, \quad (\text{left})\,; \quad U_{3yy} \sim -\varepsilon(2wU_0V_{3R} - 2Aw^2U_2(L))\,, \quad (\text{right})\,.$$

We use the matching conditions $u_{3x}(0^+) = \lim_{y\to\infty} \varepsilon^{-1}U_{3y}$ and $u_{3x}(L^-) = -\lim_{y\to\infty} \varepsilon^{-1}U_{3y}$ for the left and right boundary layers, respectively. In this way, from the u_3 equation in (3.7) we obtain that the outer solution $u_3(x)$ satisfies

(3.25a)
$$\begin{gathered} u_{3xx} - \mu_c u_3 = \tau_0 u_{1T} - ku_1 \equiv \gamma(T) g(x)\,, \quad 0 < x < L\,; \qquad u_3(0) = U_3(0)\,, \quad u_3(L) = U_3(L)\,, \\ u_{3x}(0^+) = -\left(2U_0 \int_0^\infty wV_{3L}\,dy + 2bAU_2(0)\right), \quad u_{3x}(L^-) = \left(2U_0 \int_0^\infty wV_{3R}\,dy - 2bAU_2(L)\right). \end{gathered}$$

By using (3.12) for u_1, we have that $\gamma(T)$ and $g(x)$ in (3.25a) are defined by

$$\gamma(T) \equiv \frac{1}{2}\left(\tau_0 A' - kA\right), \qquad g(x) \equiv \cosh\left[\sqrt{\mu_c}(L-x)\right] - \cosh(\sqrt{\mu_c}x)\,. \tag{3.25b}$$

The solution to (3.25a) can be decomposed as

$$u_3(x) = u_{3p}(x) - \alpha_L \frac{\sinh\left[\sqrt{\mu_c}(L-x)\right]}{\sinh(\sqrt{\mu_c}L)} + \alpha_R \frac{\sinh\left(\sqrt{\mu_c}x\right)}{\sinh(\sqrt{\mu_c}L)}\,, \tag{3.26a}$$

where the particular solution $u_{3p}(x)$, which is odd about $x = L/2$, is calculated as

$$u_{3p}(x) = -\frac{\gamma(T)\,(x - L/2)}{2\sqrt{\mu_c}}\left(\sinh\left[\sqrt{\mu_c}(L-x)\right] + \sinh(\sqrt{\mu_c}x)\right). \tag{3.26b}$$

We substitute (3.26b) into the boundary conditions in (3.25a) and, after some straightforward but lengthy algebra, we obtain that

$$\begin{pmatrix} \alpha_L \\ \alpha_R \end{pmatrix} = u_{3p}(0) \begin{pmatrix} 1 \\ 1 \end{pmatrix} + \begin{pmatrix} -U_3(0) \\ U_3(L) \end{pmatrix}, \tag{3.27a}$$

where $U_3(0)$ and $U_3(L)$ satisfy

$$\begin{pmatrix} U_3(0) \\ U_3(L) \end{pmatrix} = \left(u_{3p}(0) - \frac{\beta_0}{\kappa_+}\right)\begin{pmatrix} 1 \\ -1 \end{pmatrix} + \frac{2}{b}\tanh\left(\frac{\sqrt{\mu_c}L}{2}\right)\mathcal{P}\mathcal{G}^{-1}\mathcal{P}\begin{pmatrix} \int_0^\infty wV_{3L}\,dy \\ \int_0^\infty wV_{3R}\,dy \end{pmatrix}, \tag{3.27b}$$

where $\mathcal{G}$ is the Green's matrix of (3.19b). Here $\kappa_+ = \coth\left(\sqrt{\mu_c}L/2\right)$ is obtained from the matrix eigenvalue problem $\mathcal{G}\mathbf{e} = \kappa_+\mathbf{e}$, where $\mathbf{e} = (1,1)^T$, while β_0 and the matrix $\mathcal{P}$ are defined by

$$\beta_0 \equiv -\frac{[2bAU_2(0) + u_{3px}(0)]}{\sqrt{\mu_c}}\,, \qquad \mathcal{P} \equiv \begin{pmatrix} -1 & 0 \\ 0 & 1 \end{pmatrix}. \tag{3.27c}$$

Finally, we substitute (3.27b) into (3.23) to obtain a vector-valued NLEP for $\mathbf{V}_3 \equiv (V_{3L}, V_{3R})^T$:

$$L_0\mathbf{V}_3 - 2w^2 \tanh\left(\frac{\sqrt{\mu_c}L}{2}\right) \mathcal{P}\mathcal{G}^{-1}\mathcal{P} \frac{\int_0^\infty w\mathbf{V}_3\, dy}{\int_0^\infty w^2\, dy} = \left[wA' + w^2\left(u_{3p}(0) - \frac{\beta_0}{\kappa_+}\right)\right] \begin{pmatrix} 1 \\ -1 \end{pmatrix}. \tag{3.28}$$

3.1. The Solvability Condition and the Amplitude Equation. To determine the solvability condition, leading to the amplitude equation, we need to diagonalize (3.28). To do so, we first diagonalize $\mathcal{G}$ and introduce a new variable $\mathbf{\Psi}$ by

(3.29a)

$$\mathcal{G} = \mathcal{Q}\Lambda\mathcal{Q}^{-1}\,, \quad \mathcal{Q} \equiv \begin{pmatrix} 1 & 1 \\ 1 & -1 \end{pmatrix}, \quad \mathbf{\Psi} \equiv \mathcal{Q}^{-1}\mathcal{P}\mathbf{V}_3 = -\frac{1}{2}\begin{pmatrix} V_{3L} - V_{3R} \\ V_{3L} + V_{3R} \end{pmatrix}, \quad \mathcal{Q}^{-1}\mathcal{P}\begin{pmatrix} 1 \\ -1 \end{pmatrix} = \begin{pmatrix} 1 \\ 0 \end{pmatrix}.$$

Here the matrix of eigenvalues of $\mathcal{G}$ is

$$\Lambda \equiv \begin{pmatrix} \kappa_+ & 0 \\ 0 & \kappa_- \end{pmatrix}, \qquad \kappa_+ = \coth\left(\frac{\sqrt{\mu_c}L}{2}\right), \qquad \kappa_- = \tanh\left(\frac{\sqrt{\mu_c}L}{2}\right). \tag{3.29b}$$

We multiply both sides of (3.28) by $\mathcal{Q}^{-1}\mathcal{P}$ and use $\mathcal{P}^2 = I$ together with (3.29a) to obtain

$$L_0\mathbf{\Psi} - 2w^2 \tanh\left(\frac{\sqrt{\mu_c}L}{2}\right) \Lambda^{-1} \frac{\int_0^\infty w\mathbf{\Psi}\, dy}{\int_0^\infty w^2\, dy} = -\left[wA' + w^2\left(u_{3p}(0) - \frac{\beta_0}{\kappa_+}\right)\right] \begin{pmatrix} 1 \\ 0 \end{pmatrix}, \tag{3.30}$$

with $\mathbf{\Psi}'(0) = 0$ and $\mathbf{\Psi} \to 0$ as $y \to \infty$. In this diagonalized NLEP (3.30), $\mathbf{\Psi} \equiv (\Psi_1, \Psi_2)^T$ with $\Psi_1 = (V_{3R} - V_{3L})/2$ and $\Psi_2 = -(V_{3R} + V_{3L})/2$.

For the second component in (3.30) we obtain that

$$L_0\Psi_2 - 2w^2 \frac{\int_0^\infty w\Psi_2\, dy}{\int_0^\infty w^2\, dy} = 0\,. \tag{3.31}$$

where we readily conclude that $\Psi_2 \equiv 0$, and consequently $V_{3L} = -V_{3R}$ is the only solution. For the first component we use $\left[\tanh\left(\sqrt{\mu_c}L/2\right)\right]^2 = 1/2$ to obtain that

$$\mathcal{L}\Psi_1 \equiv L_0\Psi_1 - w^2 \frac{\int_0^\infty w\Psi_1\, dy}{\int_0^\infty w^2\, dy} = \mathcal{R} \equiv -\left[wA' + w^2\left(u_{3p}(0) - \frac{\beta_0}{\kappa_+}\right)\right]. \tag{3.32}$$

To determine the solvability condition for (3.32) we observe that the homogeneous adjoint problem

$$\mathcal{L}^\star\Psi^\star \equiv L_0\Psi^\star - w\frac{\int_0^\infty w^2\Psi^\star\, dy}{\int_0^\infty w^2\, dy} = 0\,, \tag{3.33a}$$

has the nontrivial solution $\mathcal{L}^\star\Psi_c^\star = 0$ given explicitly by (cf. [31])

$$\Psi_c^\star \equiv w + \frac{yw'}{2}\,. \tag{3.33b}$$

As such, the solvability condition for (3.32) is that $\int_0^\infty \Psi_c^\star\mathcal{R}\, dy = 0$, which yields

$$A' = \left(\frac{\beta_0}{\kappa_+} - u_{3p}(0)\right)\left(\frac{\int_0^\infty w^2\Psi_c^\star\, dy}{\int_0^\infty w\Psi_c^\star\, dy}\right). \tag{3.34}$$

Upon integrating by parts, we use (2.3) for w to calculate the integral ratio in (3.34) as

$$\frac{\int_0^\infty w^2 \Psi_c^\star \, dy}{\int_0^\infty w \Psi_c^\star \, dy} = \frac{\int_0^\infty w^2 \left(w + y w'/2\right) \, dy}{\int_0^\infty w \left(w + y w'/2\right) \, dy} = \frac{(5/6) \int_0^\infty w^3 \, dy}{(3/4) \int_0^\infty w^2 \, dy} = \frac{4}{3} \,, \tag{3.35}$$

where we used $\int_0^\infty w^3 \, dy / \int_0^\infty w^2 \, dy = 6/5$. Then, from (3.34) and together with (3.27c) for β_0 and (3.29b) for κ_+ we conclude that, with $U_0 = \sqrt{\mu_c}/(\sqrt{2} b)$,

$$A' = \frac{4}{3} \left[\frac{\beta_0}{\kappa_+} - u_{3p}(0) \right] \,, \qquad \frac{\beta_0}{\kappa_+} = \frac{\tanh\left(\sqrt{\mu_c} L/2\right)}{\sqrt{\mu_c}} \left[\frac{kA}{4} \left(L + \frac{2\sqrt{2}}{\sqrt{\mu_c}} \right) + \frac{2bA^3}{U_0} - u_{3px}(0) \right] . \tag{3.36}$$

The final step in the derivation of an explicit amplitude equation is to calculate $u_{3p}(0)$ and $u_{3px}(0)$ using (3.26b), as is needed in (3.36). We obtain that

$$\begin{aligned} u_{3p}(0) &= \frac{L}{8\sqrt{\mu_c}} \left(\tau_0 A' - kA\right) \sinh(\sqrt{\mu_c} L) = \frac{\sqrt{2} L}{4\sqrt{\mu_c}} \left(\tau_0 A' - kA\right) \,, \\ u_{3px}(0) &= \frac{(kA - \tau_0 A')}{4\sqrt{\mu_c}} \left[\sinh(\sqrt{\mu_c} L) - \frac{L\sqrt{\mu_c}}{2} \left(1 - \cosh(\sqrt{\mu_c} L)\right) \right] = \frac{(kA - \tau_0 A')}{2\sqrt{\mu_c}} \left(\sqrt{2} + \frac{L\sqrt{\mu_c}}{2} \right) . \end{aligned} \tag{3.37}$$

In obtaining (3.37) we used $\sinh(\sqrt{\mu_c} L/2) = 1$, $\sinh(\sqrt{\mu_c} L) = 2\sqrt{2}$ and $\cosh(\sqrt{\mu_c} L) = 3$.

Upon substituting (3.37) into (3.36) and solving for A' we obtain an explicit amplitude equation. The result is summarized as follows:

PROPOSITION 1. *Consider a small amplitude perturbation of a symmetric two-boundary spike steady-state solution of (1.1) for $\mu = \mu_c - k\sigma^2$, where $k = \pm 1$ and $\mu_c = 4L^{-2} \left[\ln(1+\sqrt{2})\right]^2$, and when $\tau_0 < \tau_{H+}(\mu_c) \approx 0.9336$. In the $\mathcal{O}(\varepsilon)$ boundary layers near $x = 0$ and $x = L$, we have for $\sigma \ll 1$ and $\varepsilon \ll 1$ that*

$$\begin{aligned} v &\sim w \left[U_0 + \sigma A(T) + \mathcal{O}(\sigma^2)\right] \,, \qquad u \sim U_0 + \sigma A(T) + \mathcal{O}(\sigma^2) \,, \qquad \textit{(left boundary layer)} \,, \\ v &\sim w \left[U_0 - \sigma A(T) + \mathcal{O}(\sigma^2)\right] \,, \qquad u \sim U_0 - \sigma A(T) + \mathcal{O}(\sigma^2) \,, \qquad \textit{(right boundary layer)} \,, \end{aligned} \tag{3.38}$$

where $U_0 = \sqrt{\mu_c}/(\sqrt{2} b)$. On the slow time-scale $T = \sigma^2 t$, the amplitude equation for $A(T)$ is

$$\frac{dA}{dT} = \frac{\theta_2}{\theta_1} A + \frac{\theta_3}{\theta_1} A^3 \,, \tag{3.39a}$$

where the coefficients in the amplitude equation are

$$\theta_1 \equiv 1 + \frac{2\tau_0}{3\mu_c} \left(\frac{\sqrt{2}}{2} \ln(1+\sqrt{2}) - 1 \right) \,, \qquad \theta_2 \equiv \frac{\sqrt{2} k L}{3\sqrt{\mu_c}} \,, \qquad \theta_3 \equiv \frac{8b^2}{3\mu_c} > 0 \,, \tag{3.39b}$$

where $k = \pm 1$ and $b \equiv \int_0^\infty w^2 \, dy = 3$. The competition instability associated with the zero-eigenvalue crossing of the NLEP for the anti-phase mode of the linearization around the symmetric two-boundary steady state is subcritical.

On the range $\tau_0 < \tau_{H+}(\mu_c) < \tau_{H-}(\mu_c)$ we have $\theta_1 > 0$. In fact, by comparing the expression for θ_1 in (3.39b) with the Hopf bifurcation threshold $\tau_{H-}(\mu_c)$ for the anti-phase mode given in (2.19), we observe that $\theta_1 > 0$ on $0 < \tau_0 < \tau_{H+}(\mu_c) < \tau_{H-}(\mu_c)$, and that $\theta_1 = 0$ precisely when $\tau_0 = \tau_{H-}$. From the amplitude equation (3.39a) we obtain that the equilibrium $A_e = 0$ is unstable when $\mu = \mu_c - \sigma^2$ $(k = 1)$ and is linearly stable when $\mu = \mu_c + \sigma^2$ $(k = -1)$. As shown in Appendix B, the growth rate

θ_2/θ_1 is consistent with that obtained by calculating for $\sigma \ll 1$ the near-zero eigenvalue of the NLEP (2.16) for the anti-phase mode when $\mu = \mu_c - \sigma^2$.

On the range $\mu = \mu_c + \sigma^2$ where $A_e = 0$ is linearly stable, there are unstable steady-state $A_{e\pm}$ of the amplitude equation (3.39a) given by $A_{e\pm} = \pm\sqrt{\theta_2/\theta_3}$. By calculating the ratio θ_2/θ_3 for $k = -1$, we observe that this steady-state corresponds to the emergence of a linearly unstable asymmetric two-boundary spike steady-state solution u_e, for which in the two boundary layers we have

$$u_e \sim U_0 \pm \frac{\sqrt{\mu - \mu_c}}{b}\sqrt{\frac{\sqrt{2u_c}L}{8}} \text{ (left layer)}\,; \qquad u_e \sim U_0 \mp \frac{\sqrt{\mu - \mu_c}}{b}\sqrt{\frac{\sqrt{2u_c}L}{8}} \text{ (right layer)}\,, \tag{3.40}$$

when $\mu = \mu_c + \sigma^2$ and $U_0 = \sqrt{\mu_c}/(\sqrt{2}b)$. This weakly nonlinear analysis shows that the competition instability for a symmetric two-boundary spike steady-state that occurs at $\mu = \mu_c$ is subcritical.

3.2. Asymmetric Boundary Spike Equilibria. We now construct global branches of asymmetric two-boundary spike steady-state solutions of (1.1) for $\varepsilon \ll 1$. We show that these asymmetric equilibria bifurcate from the symmetric two-boundary spike branch at $\mu = \mu_c$, and near the bifurcation point their local behavior agrees with (3.40), as was obtained from our weakly nonlinear analysis.

In the left boundary layer near $x = 0$ we have $v \sim U_L w$ and $u = U_L + \mathcal{O}(\varepsilon)$, while in the right boundary layer near $x = L$, we have $v \sim U_R w$ and $u = U_R + \mathcal{O}(\varepsilon)$. Proceeding as in the matched asymptotic analysis of symmetric two-boundary spike equilibria in §2, we obtain in the outer region that the leading-order inhibitor field satisfies

$$u_{xx} - \mu u = 0\,, \quad 0 < x < L\,; \qquad u_x(0^+) = -U_L^2 b\,, \quad u_x(L^-) = U_R^2 b\,, \tag{3.41}$$

where $b \equiv \int_0^\infty w^2\,dy$, $u(0^+) = U_L$, and $u(L^-) = U_R$. The explicit solution to (3.41) is

$$u(x) = U_L \frac{\sinh(\sqrt{\mu}(L - x))}{\sinh(\sqrt{\mu}L)} + U_R \frac{\sinh(\sqrt{\mu}x)}{\sinh(\sqrt{\mu}L)}\,. \tag{3.42}$$

Then, by satisfying the flux boundary conditions, we obtain the nonlinear algebraic system

$$\begin{pmatrix} z_L^2 \\ z_R^2 \end{pmatrix} = \mathcal{A} \begin{pmatrix} z_L \\ z_R \end{pmatrix}\,, \qquad \text{with} \qquad \mathcal{A} \equiv \begin{pmatrix} \coth(\sqrt{\mu}L) & -\operatorname{csch}(\sqrt{\mu}L) \\ -\operatorname{csch}(\sqrt{\mu}L) & \coth(\sqrt{\mu}L) \end{pmatrix}\,, \tag{3.43a}$$

where z_L and z_R are related to U_L and U_R by

$$U_L = \frac{\sqrt{\mu}}{b} z_L\,, \qquad U_R = \frac{\sqrt{\mu}}{b} z_R\,. \tag{3.43b}$$

The symmetric two-boundary spike solution is obtained by setting $\mathbf{z} \equiv (z_L, z_R)^T = z_c(1,1)^T$. Since $\mathcal{A}$ is a cyclic symmetric matrix, $\mathbf{e} \equiv (1,1)^T$ is an eigenvector and we obtain

$$U_L = U_R = \frac{\sqrt{\mu} z_c}{b}\,, \quad \text{where} \quad z_c = \tanh\left(\frac{\sqrt{\mu}L}{2}\right) \quad \text{and} \quad \mathcal{A}\mathbf{e} = \tanh\left(\frac{\sqrt{\mu}L}{2}\right)\mathbf{e}\,. \tag{3.44}$$

Next, we linearize (3.43a) about $\mathbf{z} = z_c\mathbf{e}$ by writing $\mathbf{z} = z_c\mathbf{e} + \eta$, where $|\eta| \ll 1$. From (3.43a) we obtain the linearized problem $\mathcal{A}\eta = 2z_c\eta$. Since $\mathcal{A}\mathbf{q} = \coth\left(\sqrt{\mu}L/2\right)\mathbf{q}$, where $\mathbf{q} = (1,-1)^T$, we conclude that $\eta = (1,-1)^T$ is a nontrivial solution to the linearized problem provided that $2z_c = \coth\left(\sqrt{\mu}L/2\right)$. This determines a critical value $\mu = \mu_c$. By using (3.44) for z_c, we conclude that $\sinh\left(\sqrt{\mu_c}L/2\right) = 1$, which yields $\sqrt{\mu_c}L = 2\ln(1+\sqrt{2})$. This critical value of μ, where asymmetric two-boundary spike steady-states emerge from the symmetric branch, coincides with the zero-eigenvalue crossing of the NLEP (2.16) for the anti-phase mode, as was analyzed in §2.1.

To calculate global branches of asymmetric two-boundary spike equilibria, we rewrite (3.43a) as

$$z_L^2+z_R^2 = k_2(z_L+z_R)\,, \quad z_L^2-z_R^2 = k_1(z_L-z_R)\,; \quad k_1 \equiv \coth\left(\frac{\sqrt{\mu}L}{2}\right)\,, \quad k_2 \equiv \tanh\left(\frac{\sqrt{\mu}L}{2}\right)\,. \tag{3.45}$$

From the second equation in (3.45) we observe that for asymmetric equilibria where $z_L \neq z_R$, we must have $z_L + z_R = k_1$. Upon substituting this relation into the first equation of (3.45) we conclude that z_L and z_R must be the roots of the quadratic $2z^2 - 2k_1 z + k_1^2 - k_1k_2 = 0$. In this way, and upon calculating $2k_1k_2 - k_1^2 = 2 - k_1^2$, the global branches of asymmetric two-boundary spike equilibria are characterized by

$$\begin{pmatrix} U_L \\ U_R \end{pmatrix} = \frac{\sqrt{\mu}}{b}\begin{pmatrix} z_L \\ z_R \end{pmatrix}\,, \quad z_L = \frac{1}{2}\left(k_1 \pm \sqrt{2-k_1^2}\right)\,, \quad z_R = \frac{1}{2}\left(k_1 \mp \sqrt{2-k_1^2}\right)\,, \tag{3.46}$$

provided that $\mu > \mu_c$. As $\mu \to \mu_c$ from above, we remark that a straightforward Taylor series expansion, together with the identity $\tanh\left(\sqrt{\mu_c}L/2\right) = 1/\sqrt{2}$, shows that U_L and U_R reduce to

$$U_R \sim \frac{\sqrt{\mu_c}}{\sqrt{2}b} \pm \frac{1}{b}\sqrt{\frac{\sqrt{2\mu_c}L}{8}}\sqrt{\mu-\mu_c} + \mathcal{O}((\mu-\mu_c))\,; \quad U_L \sim \frac{\sqrt{\mu_c}}{\sqrt{2}b} \mp \frac{1}{b}\sqrt{\frac{\sqrt{2\mu_c}L}{8}}\sqrt{\mu-\mu_c} + \mathcal{O}((\mu-\mu_c))\,. \tag{3.47}$$

This recovers the result given in (3.40) from the amplitude equation of the weakly nonlinear theory.

In the right panel of Fig. 4 we plot global branches of asymmetric two-boundary spike equilibria versus μ as obtained from (3.46) when $L = 2$. The symmetric branch, as given in (3.44), is also shown. The dashed-dotted curves in this figure are the steady-state results (3.40) from the amplitude equation obtained from the weakly nonlinear theory, which is valid near the bifurcation point. In the left panel of Fig. 4 we plot an asymmetric two-boundary spike solution when $\mu = 1.0$ and $L = 2$.

In Fig. 5 we plot numerically-computed bifurcation branches of symmetric and asymmetric two-boundary spike equilibria for the GM model versus μ when $L = 2$ and $\varepsilon = 0.01$, as computed using the bifurcation software COCO [4] upon discretizing the steady-state of (1.1) with $N = 800$ mesh points. As shown in Fig. 4, the prediction (3.47) of the weakly nonlinear theory compares favorably with these full numerical bifurcation results.

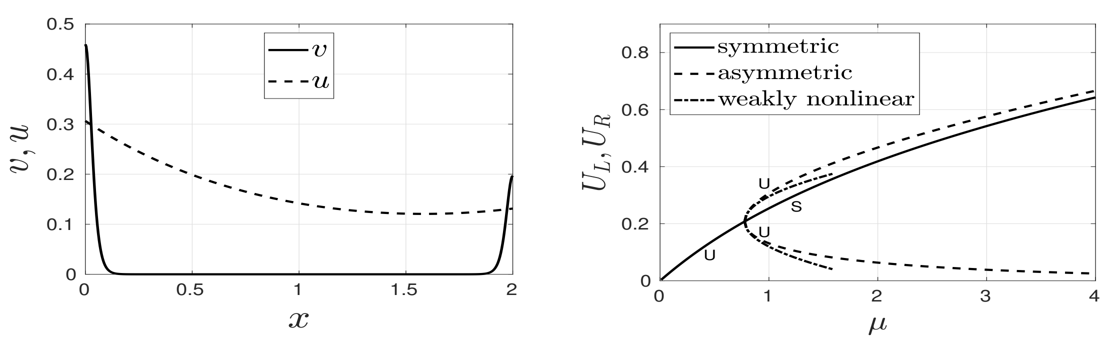

FIG. 4. *Left panel: The asymmetric two-boundary spike solution for $L = 2$, $\varepsilon = 0.02$, and $\mu = 1.0$ with u as given in (3.42) and $v \sim U_L w(\varepsilon^{-1}x) + U_R w(\varepsilon^{-1}(L-x))$, where $w(y)$ is the homoclinic in (2.3). Right panel: Global branches of asymmetric and symmetric two-boundary spike equilibria obtained from (3.46) and (3.44), respectively, together with the local behavior in (3.40) predicted from the weakly nonlinear theory for $L = 2$ and $\varepsilon = 0.02$. Linear stability results are indicated.*

4. Schnakenberg Model. In this section we perform a similar weakly nonlinear analysis to show that a competition instability of a symmetric two-boundary spike steady-state solution to the

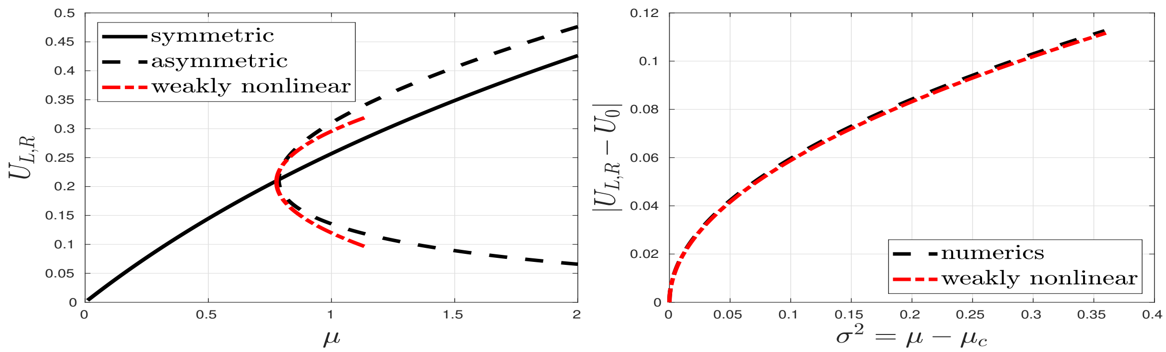

FIG. 5. *Left panel: Numerical bifurcation branches of symmetric (full black curve) and asymmetric (dashed black curve) two-boundary spike equilibria for the GM model versus μ, as computed with* COCO *[4] upon discretizing the steady-state of the PDE system* (1.1) *with $N = 800$ mesh points. The dot-dashed red curve is the weakly nonlinear prediction* (3.47) *for the asymmetric pattern. Parameters are $L = 2$ and $\varepsilon = 0.01$. Right panel: A zoomed-in view of the amplitude of the asymmetric equilibria shifted to the origin.*

Schnakenberg model (1.2) is subcritical. After first using boundary layer theory to construct such a steady-state, in §4.1 an NLEP linear stability analysis is developed to determine a critical value of μ in (1.2) for the onset of the competition instability. A weakly nonlinear theory, valid near this threshold, and that reveals the subcritical behavior is presented in §4.1.

We first use the method of matched asymptotic expansions to construct symmetric two-boundary spike equilibria for (1.2). In the boundary layer region near $x = 0$ we let $u(\varepsilon y) = U = U_0 + \varepsilon U_1 + \ldots$ and $v(\varepsilon y) = V_0 + \varepsilon V_1 + \ldots$, where $y = x/\varepsilon$. We obtain that U_0 is a constant and that

$$V_{0yy} - V_0 + U_0 V_0^2 = 0\,, \qquad U_{1yy} = U_0 V_0^2\,, \qquad y \geq 0\,, \tag{4.1}$$

with $V_{0y} = U_{1y} = 0$ at $y = 0$. We conclude that $V_0 = w(y)/U_0$, where $w(y)$ is the homoclinic in (2.3). From integrating the U_1 equation in (4.1) we get $U_y \sim \varepsilon U_{1y} = \varepsilon b/U_0$ where $b \equiv \int_0^\infty w^2\, dy$, which provides the matching condition for the outer solution as $x \to 0^+$. A similar boundary layer analysis can be done near $x = L$. In the outer region, v is exponentially small, while from the steady-state of (1.2), together with the matching conditions to the boundary layer solution, we obtain that the leading-order outer solution for u satisfies

$$u_{xx} = -\mu\,, \quad 0 < x < L\,; \qquad u_x(0^+) = \frac{b}{U_0}\,, \quad u_x(L^-) = -\frac{b}{U_0}\,, \tag{4.2}$$

with $u(0^+) = u(L^-) = U_0$. The solution to (4.2) is

$$u = \frac{\mu L x}{2}\left(1 - \frac{x}{L}\right) + U_0\,, \quad 0 < x < L\,; \qquad \text{where} \qquad U_0 = \frac{2b}{\mu L}\,, \quad b \equiv \int_0^\infty w^2\, dy\,. \tag{4.3}$$

4.1. Linear Stability Analysis. We now derive the NLEP governing the linear stability of the symmetric two-boundary spike steady-state, denoted by $v = v_e$ and $u = u_e$. We set $v = v_e + e^{\lambda t}\phi(x)$ and $u = u_e + e^{\lambda t}\eta(x)$ in (1.2) and, upon linearization, obtain the eigenvalue problem

$$\varepsilon^2 \phi_{xx} - \phi + 2 v_e u_e \phi + v_e^2 \eta = \lambda \phi\,, \quad 0 < x < L\,; \qquad \phi_x = 0 \quad \text{at } x = 0, L\,, \tag{4.4a}$$

$$\eta_{xx} - \tau_0 \lambda \eta = \varepsilon^{-1}\left(2 v_e u_e \phi + v_e^2 \eta\right)\,, \quad 0 < x < L\,; \qquad \eta_x = 0 \quad \text{at } x = 0, L\,. \tag{4.4b}$$

We look for a localized eigenfunction for (4.4a) in the form (2.7). From (4.4a), $\Phi(y)$ satisfies

$$c_j L_0 \Phi + \eta(x_j)\frac{w^2}{U_0^2} = \lambda c_j \Phi\,, \qquad 0 \leq y < \infty\,, \qquad \text{where} \qquad L_0\Phi \equiv \Phi_{yy} - \Phi + 2w\Phi\,. \tag{4.5}$$

Here $\eta(x_1)$ and $\eta(x_2)$ are the unknown constant leading-order approximations for $\eta(x)$ near $x_1 \equiv 0$ and $x_2 \equiv L$, $U_0 = 2b/(\mu L)$, and w is the homoclinic given in (2.3). In the boundary layers near $x = x_j$ for $j = 1, 2$, we expand $\eta = \eta(x_j) + \varepsilon\eta_1(y) + \ldots$, with $y = x/\varepsilon$ for $j = 1$ and $y = \varepsilon^{-1}(L - x)$ for $j = 2$. Upon collecting $\mathcal{O}(\varepsilon^{-1})$ terms in (4.4b), and using $v_e \sim w/U_0$ and $u_e \sim U_0$, we get

$$\eta_{1yy} = 2wc_j\Phi + \eta(x_j)\frac{w^2}{U_0^2}\,, \quad 0 \le y < \infty\,; \qquad \eta_{1y}(x_j) = 0\,. \tag{4.6}$$

By integrating (4.6) over $0 < y < \infty$ we obtain the matching conditions for the flux of the outer solution as $x \to 0^+$ and $x \to L^-$. In this way, we obtain that the leading-order outer solution $N_0(x)$ for (4.4b) satisfies

$$\begin{aligned} &N_{0xx} - \tau_0\lambda N_0 = 0\,, \quad 0 < x < L\,; \qquad N_0(0^+) = \eta(0)\,, \quad N_0(L^-) = \eta(L)\,, \\ &N_{0x}(0^+) = 2c_1\int_0^\infty w\Phi\,dy + \frac{b}{U_0^2}\eta(0)\,, \qquad N_{0x}(L^-) = -2c_2U_0\int_0^\infty w\Phi\,dy - \frac{b}{U_0^2}\eta(L)\,. \end{aligned} \tag{4.7}$$

The solution to (4.7) is given in (2.12) upon replacing θ_λ in (2.12) with $\theta_\lambda = \sqrt{\tau_0\lambda}$. We then set $N(0^+) = \eta(0)$ and $N(L^-) = \eta(L)$ and, after some algebra, derive that

$$\begin{pmatrix} \eta(0) \\ \eta(L) \end{pmatrix} = -\frac{2\int_0^\infty w\Phi\,dy}{\theta_\lambda}\left(I + \frac{b}{\theta_\lambda U_0^2}\mathcal{G}_\lambda\right)^{-1}\mathcal{G}_\lambda\begin{pmatrix} c_1 \\ c_2 \end{pmatrix}, \tag{4.8}$$

where the 2×2 symmetric Green's matrix $\mathcal{G}_\lambda$ is defined in (2.13b) in terms of $\theta_\lambda = \sqrt{\tau_0\lambda}$. Upon substituting (4.8) into (4.5) and defining $\mathbf{c} \equiv (c_1, c_2)^T$, we obtain the vector-valued NLEP

$$(L_0\Phi)\,\mathbf{c} - \frac{2bw^2}{U_0^2\theta_\lambda}\left(\frac{\int_0^\infty w\Phi\,dy}{\int_0^\infty w^2\,dy}\right)\left(I + \frac{b}{\theta_\lambda U_0^2}\mathcal{G}_\lambda\right)^{-1}\mathcal{G}_\lambda\mathbf{c} = \lambda\Phi\mathbf{c}\,. \tag{4.9}$$

To obtain two scalar NLEPs from (4.9), we diagonalize $\mathcal{G}_\lambda$ and introduce $\hat{\mathbf{c}}$ by

$$\mathcal{G}_\lambda = \mathcal{Q}\Lambda\mathcal{Q}^{-1}\,, \quad \mathcal{Q} \equiv \begin{pmatrix} 1 & 1 \\ 1 & -1 \end{pmatrix}, \quad \Lambda \equiv \begin{pmatrix} \kappa_+ & 0 \\ 0 & \kappa_- \end{pmatrix}, \quad \hat{\mathbf{c}} \equiv \mathcal{Q}^{-1}\mathbf{c} = \frac{1}{2}\begin{pmatrix} c_1 + c_2 \\ c_1 - c_2 \end{pmatrix}, \tag{4.10a}$$

where $\kappa_+ = \coth(\theta_\lambda L/2)$ and $\kappa_- = \tanh(\theta_\lambda L/2)$. We then calculate

$$(I + z\mathcal{G}_\lambda)^{-1}\mathcal{G}_\lambda = \mathcal{Q}\mathcal{D}\mathcal{Q}^{-1}\,, \qquad \mathcal{D} \equiv \begin{pmatrix} \frac{\kappa_+}{(1+z\kappa_+)} & 0 \\ 0 & \frac{\kappa_-}{(1+z\kappa_-)} \end{pmatrix}, \quad \text{where} \quad z \equiv \frac{b}{\theta_\lambda U_0^2}\,. \tag{4.10b}$$

Upon substituting (4.10) into (4.9) we obtain the following scalar NLEPs for the in-phase $(+)$ mode, where $\mathbf{c} = (1,1)^T$, and for the anti-phase $(-)$ mode, where $\mathbf{c} = (1,-1)^T$:

$$L_0\Phi - \chi_\pm(\lambda,\mu)w^2\left(\frac{\int_0^\infty w\Phi\,dy}{\int_0^\infty w^2\,dy}\right) = \lambda\Phi\,, \quad y \ge 0\,; \qquad \Phi_y(0) = 0\,, \quad \lim_{y\to\infty}\Phi(y) = 0\,. \tag{4.11a}$$

In terms of $\theta_\lambda = \sqrt{\tau_0\lambda}$, and with $U_0 = 2b/(\mu L)$, the NLEP multipliers $\chi_\pm(\lambda,\mu)$ are defined by

$$\chi_+(\lambda,\mu) \equiv \frac{2}{1 + \frac{U_0^2}{b}\theta_\lambda\tanh(\theta_\lambda L/2)}\,, \qquad \chi_-(\lambda,\mu) \equiv \frac{2}{1 + \frac{U_0^2}{b}\theta_\lambda\coth(\theta_\lambda L/2)}\,. \tag{4.11b}$$

Since the analysis of these NLEPs is similar to that in [29] and [22], we now only briefly summarize the main results for the spectrum of (2.16).

For the in-phase mode, we have $\mathrm{Re}(\lambda) < 0$ only when $\tau_0 < \tau_{H+}(\mu)$. For the anti-phase mode, there is an unstable real positive eigenvalue of the NLEP for any $\tau_0 \geq 0$ whenever $\mu < \mu_c$ where $\mu_c \equiv \sqrt{8b/L^3}$. This critical value is obtained from $\chi_-(0, \mu) = 1$, $\lambda = 0$ and $\Phi = w$. When $\mu > \mu_c$, there is a Hopf bifurcation at $\tau = \tau_{H-}(\mu)$ and $\lambda = \pm i\lambda_{IH-}(\mu)$. As $\mu \to \mu_c$ from above, we have $\lambda_{IH-}(\mu) \to 0$. In Appendix C we show that the Hopf curves $\tau_{H\pm} = \tau_{H\pm}(\mu)$ can be computed numerically by using a scaling law that is valid for all domain lengths L. For $L = 2$, in Fig. 6 we plot the Hopf bifurcation curves for both the in-phase and anti-phase modes in the τ_0 versus μ plane. In particular, we calculate

$$\tau_{H+} \approx 0.906\,, \qquad \tau_{H-} = \frac{18}{L^2} = 4.5\,, \tag{4.12}$$

when $\mu = \mu_c \approx 1.732$ and $L = 2$. In Appendix C we derive this explicit result for τ_{H-} when $\mu = \mu_c$.

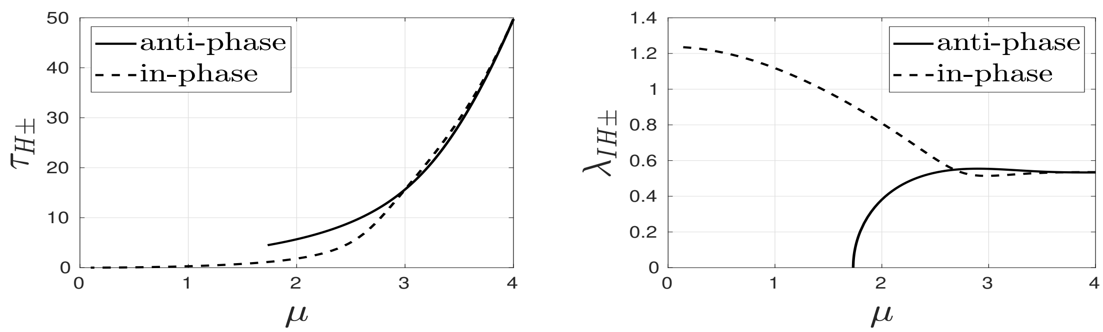

FIG. 6. *Spectral results from NLEP theory for the linearization of symmetric two-boundary spike equilibria for the Schnakenberg model (1.2). Numerically computed Hopf bifurcation thresholds $\tau_{H\pm}$ (left panel) and corresponding imaginary parts $\lambda_{IH\pm}$ (right panel) of the eigenvalues versus μ when $L = 2$, as computed using Newton's method on (C.1), for both the in-phase (+) and anti-phase (−) modes. The Hopf threshold for the anti-phase mode exists only when $\mu > \mu_c$, where $\mu_c = \sqrt{8b/L^3}$. For $L = 2$, as μ tends to $\mu_c \approx 1.73$ from above we have $\tau_{H-} \to 4.5$ and $\lambda_{IH-} \to 0$. At $\mu = \mu_c$, the Hopf threshold for the in-phase mode is $\tau_{H+} \approx 0.906$. For any $\mu < \mu_c$, the anti-phase mode is always unstable due to a positive real eigenvalue for the NLEP. For $\mu > \mu_c$, the symmetric two-boundary spike steady-state is linearly stable only when $\tau_0 < \min(\tau_{H-}, \tau_H+)$.*

4.2. Weakly Nonlinear Analysis. We now perform a weakly nonlinear analysis near the zero-eigenvalue crossing at $\mu = \mu_c$ when $0 \leq \tau_0 < \min(\tau_{H+}(\mu_c), \tau_{H-}(\mu_c)) = \tau_{H+}(\mu_c)$. For $\sigma \ll 1$, we introduce a neighborhood near μ_c and a slow time scale T by

$$\mu = \mu_c - k\sigma^2\,, \qquad k = \pm 1\,, \qquad \mu_c \equiv \sqrt{\frac{8b}{L^3}}\,; \qquad T = \sigma^2 t\,. \tag{4.13}$$

We obtain from (1.2) that $v(x,T)$ and $u(x,T)$, with $u_x = v_x = 0$ at $x = 0$ and $x = L$, satisfies

$$\sigma^2 v_T = \varepsilon^2 v_{xx} - v + uv^2\,, \qquad \tau_0\sigma^2 u_T = u_{xx} + (\mu_c - k\sigma^2)u - \varepsilon^{-1}uv^2\,. \tag{4.14}$$

We let $v_e(x)$ and $u_e(x)$ denote the steady-state boundary spike solution and we expand as in (3.3). Upon substituting (3.3) into (4.14) we collect powers of σ to get leading order problem

$$\varepsilon^2 v_{exx} - v_e + u_e v_e^2 = 0\,, \qquad u_{exx} = -\mu_c + \varepsilon^{-1}u_e v_e^2\,, \tag{4.15}$$

on $0 < x < L$ and the following problem at order $\mathcal{O}(\sigma)$:

$$\varepsilon^2 v_{1xx} - v_1 + 2v_e u_e v_1 = -u_1 v_e^2\,, \qquad u_{1xx} = \varepsilon^{-1}\left(u_1 v_e^2 + 2v_e u_e v_1\right)\,. \tag{4.16}$$

From the $\mathcal{O}(\sigma^2)$ terms we obtain on $0 < x < L$ that

$$\begin{aligned} \varepsilon^2 v_{2xx} - v_2 + 2v_e u_e v_2 &= -u_2 v_e^2 - u_e v_1^2 - 2u_1 v_1 v_e \,, \\ u_{2xx} &= k + \varepsilon^{-1}\left(u_2 v_e^2 + u_e v_1^2 + 2u_e v_e v_2 + 2v_e u_1 v_1\right) \,. \end{aligned} \tag{4.17}$$

Finally, we obtain that the problem at $\mathcal{O}(\sigma^3)$ is

$$\begin{aligned} \varepsilon^2 v_{3xx} - v_3 + 2v_e u_e v_3 &= v_{1T} - v_e^2 u_3 - 2v_e u_2 v_1 - u_1 v_1^2 - 2v_e u_1 v_2 - 2u_e v_1 v_2 \\ u_{3xx} &= \varepsilon^{-1}\left(v_e^2 u_3 + 2v_e u_2 v_1 + u_1 v_1^2 + 2v_e u_1 v_2 + 2u_e v_1 v_2 + 2u_e v_e v_3\right) + \tau_0 U_{1T} \,. \end{aligned} \tag{4.18}$$

For (4.15)–(4.18) we impose $v_{ex} = u_{ex} = 0$ at $x = 0, L$ and $v_{jx} = u_{jx} = 0$ at $x = 0, L$, for $j = 1, \ldots, 3$.

In the boundary layer near $x = 0$ or $x = L$ we have $v_e \sim V_0 \equiv w/U_0$ and $u_e \sim U_0$, where $U_0 = \sqrt{bL/2}$ when $\mu = \mu_c$ (see (4.3) and (4.13)) and $w(y)$ is the homoclinic in (2.3) with either $y = x/\varepsilon$ or $y = (L-x)/\varepsilon$. The steady-state outer solution satisfying $u_{exx} = -\mu_c$ is given by setting $\mu = \mu_c$ in (4.3). At next order, we obtain from (4.16) that in either of the two boundary layers

$$L_0 V_1 \equiv V_{1yy} - V_1 + 2wV_1 = -\frac{U_1}{U_0^2} w^2 \,, \qquad U_{1yy} = \varepsilon\left(U_1 V_0^2 + 2V_0 U_0 V_1\right) \,, \tag{4.19}$$

so that to leading-order U_1 is a constant. Since $L_0 w = w^2$, and a competition instability is due to a sign-fluctuating eigenfunction, we conclude that

$$\begin{aligned} U_1 &= -U_0^2 A + \mathcal{O}(\varepsilon) \,, \qquad V_1 = wA + \mathcal{O}(\varepsilon) \,, \quad \text{near } \; x = 0 \,; \\ U_1 &= U_0^2 A + \mathcal{O}(\varepsilon) \,, \qquad V_1 = -Aw + \mathcal{O}(\varepsilon) \,, \quad \text{near } \; x = L \,. \end{aligned} \tag{4.20}$$

Our analysis will derive an ODE for the amplitude $A = A(T)$.

From integrating the U_1 equation in (4.19), and by calculating $U_1 V_0^2 + 2U_0 V_0 V_1 \sim \pm A w^2$ in the two boundary layers, we readily obtain the following matching conditions between the outer inhibitor field u_1 and the two boundary layer solutions:

$$\begin{aligned} u_1(0^+) &= -U_0^2 A \,, \quad u_{1x}(0^+) = \lim_{y\to\infty} \varepsilon^{-1} U_{1y} = A \int_0^\infty w^2 \, dy = Ab \\ u_1(L^-) &= U_0^2 A \,, \quad u_{1x}(L^-) = -\lim_{y\to\infty} \varepsilon^{-1} U_{1y} = A \int_0^\infty w^2 \, dy = Ab \,, \end{aligned} \tag{4.21}$$

where $b = \int_0^\infty w^2 \, dy = 3$. From (4.21) and (4.16), the outer solution u_1 satisfies

$$u_{1xx} = 0 \,, \quad 0 < x < L \,; \quad u_1(0^+) = -U_0^2 A \,, \quad u_1(L^-) = U_0^2 A \,; \quad u_{1x}(0^+) = u_{1x}(L^-) = Ab \,, \tag{4.22}$$

which has the solution

$$u_1(x) = A\left(bx - U_0^2\right) \,. \tag{4.23}$$

Since $2U_0^2 = bL$, we readily verify that $u_1(L) = U_0^2 A$.

Next, we analyze the $\mathcal{O}(\sigma^2)$ system given in (4.17). We denote $V_{2L}(y)$ with $y = x/\varepsilon$ and $V_{2R}(y)$ with $y = (L-x)/\varepsilon$ to be the inner solution for v_2 in the left and right boundary layers, respectively. By using $V_1 \sim wA$ and $U_1 \sim -U_0^2 A$ in the left layer and $V_1 \sim -wA$ and $U_1 \sim U_0^2 A$ in the right layer, we readily calculate from (4.17) that

$$\begin{aligned} &L_0 V_{2L} \sim w^2\left(-\frac{U_2(0)}{U_0^2} + A^2 U_0\right) \,, \quad U_{2yy} = \varepsilon\left[\left(\frac{U_2(L)}{U_0^2} - A^2 U_0\right) w^2 + 2wV_{2L}\right] + \mathcal{O}(\varepsilon^2) \,, \quad (\text{left}) \,, \\ &L_0 V_{2R} \sim w^2\left(-\frac{U_2(L)}{U_0^2} + A^2 U_0\right) \,, \quad U_{2yy} = \varepsilon\left[\left(\frac{U_2(L)}{U_0^2} - A^2 U_0\right) w^2 + 2wV_{2R}\right] + \mathcal{O}(\varepsilon^2) \,, \quad (\text{right}) \,. \end{aligned} \tag{4.24}$$

Since $L_0 w = w^2$, we conclude that

$$V_{2L}(y) = \left(-\frac{U_2(0)}{U_0^2} + A^2 U_0\right) w(y)\,, \qquad V_{2R}(y) = \left(-\frac{U_2(L)}{U_0^2} + A^2 U_0\right) w(y)\,. \tag{4.25}$$

We then substitute (4.25) into the expressions for U_{2yy} in (4.24) and integrate over $0 < y < \infty$ to obtain asymptotic matching conditions that determine $u_{2x}(0^+)$ and $u_{2x}(L^-)$. Then, from (4.17), the outer correction u_2 satisfies

$$u_{2xx} = k\,, \quad 0 < x < L\,; \quad u_{2x}(0^+) = \left(-\frac{u_2(0)}{U_0^2} + A^2 U_0\right) b\,, \quad u_{2x}(L^-) = \left(\frac{u_2(L)}{U_0^2} - A^2 U_0\right) b\,, \tag{4.26}$$

where $U_2(0) = u_2(0)$ and $U_2(L) = u_2(L)$. The solution to (4.26) is even about $x = L/2$, and by integrating over $0 < x < L$, we obtain that $u_{2x}(L) - u_{2x}(0) = kL$. Since $u_2(0) = u_2(L)$, we get

$$U_2(0) = U_2(L) = \frac{kU_0^2 L}{2b} + A^2 U_0^3\,. \tag{4.27}$$

Upon using these expressions in (4.25), we obtain in the two boundary layers that

$$V_{2L}(y) = -\frac{L}{2b} w(y)\,, \qquad V_{2R}(y) = -\frac{L}{2b} w(y)\,. \tag{4.28}$$

Next, we derive a solvability condition from the $\mathcal{O}(\sigma^3)$ problem, given by (4.18), which determines the amplitude equation. We denote $V_{3L}(y)$, with $y = x/\varepsilon$, and $V_{3R}(y)$, with $y = (L-x)/\varepsilon$, to be the inner solution for v_3 in the left and right boundary layers, respectively. In the left and right boundary layers, we use respectively,

$$\begin{aligned} &V_0 \sim \frac{w}{U_0}\,, \quad V_1 \sim Aw\,, \quad V_2 \sim -\frac{L}{2b} w\,, \quad U_1 \sim -U_0^2 A\,, \quad U_2 \sim \frac{kU_0^2 L}{2b} + A^2 U_0^3\,, \quad U_3 \sim U_3(0)\,, \\ &V_0 \sim \frac{w}{U_0}\,, \quad V_1 \sim -Aw\,, \quad V_2 \sim -\frac{L}{2b} w\,, \quad U_1 \sim U_0^2 A\,, \quad U_2 \sim \frac{kU_0^2 L}{2b} + A^2 U_0^3\,, \quad U_3 \sim U_3(L)\,, \end{aligned}$$

to calculate that

$$U_3 V_0^2 + 2U_2 V_0 V_1 + U_1 V_1^2 + 2U_1 V_0 V_2 + 2U_0 V_1 V_2 \sim \begin{cases} U_3(0)\frac{w^2}{U_0^2} + \frac{kU_0 L}{b} Aw^2 + A^3 U_0^2 w^2\,, & \text{(left)}\,, \\ U_3(L)\frac{w^2}{U_0^2} - \frac{kU_0 L}{b} Aw^2 - A^3 U_0^2 w^2\,, & \text{(right)}\,. \end{cases} \tag{4.29}$$

We then use $V_{1T} \sim A'w$ and $V_{1T} \sim -A'w$ in the left and right boundary layers, respectively, together with (4.29), to calculate the right-hand side of the v_3 equation in (4.18) in the two boundary layers. In this way, we obtain that

$$L_0 \begin{pmatrix} V_{3L} \\ V_{3R} \end{pmatrix} + \frac{w^2}{U_0^2} \begin{pmatrix} U_3(0) \\ U_3(L) \end{pmatrix} = \left[wA' - \frac{kLU_0}{b} Aw^2 - A^3 U_0^2 w^2 \right] \begin{pmatrix} 1 \\ -1 \end{pmatrix}\,, \tag{4.30}$$

where $A' = dA/dT$. Moreover, by using (4.29) in the u_3 equation of (4.18) we obtain in the two boundary layers that

$$\begin{aligned} U_{3yy} &\sim \varepsilon \left[2wV_{3L} + \left(\frac{U_3(0)}{U_0^2} + \frac{kLU_0}{b} A + A^3 U_0^2 \right) w^2 \right] + \mathcal{O}(\varepsilon^2)\,, \quad \text{(left layer)}\,, \\ U_{3yy} &\sim \varepsilon \left[-2wV_{3R} + \left(-\frac{U_3(L)}{U_0^2} + \frac{kLU_0}{b} A + A^3 U_0^2 \right) w^2 \right] + \mathcal{O}(\varepsilon^2)\,, \quad \text{(right layer)}\,. \end{aligned} \tag{4.31}$$

Then, we use the matching conditions $u_{3x}(0^+) = \lim_{y\to\infty} \varepsilon^{-1} U_{3y}$ and $u_{3x}(L^-) = -\lim_{y\to\infty} \varepsilon^{-1} U_{3y}$ for the left and right boundary layers, respectively, to derive the boundary conditions for the outer solution $u_3(x)$. In this way, we obtain from (4.18), and upon using $U_0^2 = bL/2$ and the expression (4.23) for u_1, that u_3 with $u_3(0) = U_3(0)$ and $u_3(L) = U_3(L)$ satisfies

$$\begin{aligned} u_{3xx} &= \tau_0 u_{1T} = \tau_0 A' b \left(x - \frac{L}{2} \right), \quad 0 < x < L\,, \\ u_{3x}(0^+) &= 2\int_0^\infty w V_{3L}\, dy + \frac{2}{L} U_3(0) + kLU_0 A + \frac{b^2 L}{2} A^3\,, \\ u_{3x}(L^-) &= -2\int_0^\infty w V_{3R}\, dy - \frac{2}{L} U_3(L) + kLU_0 A + \frac{b^2 L}{2} A^3\,. \end{aligned} \tag{4.32}$$

Next, we calculate $U_3(0)$ and $U_3(L)$, which is used to determine the vector-valued NLEP from (4.30). We derive a linear algebraic system for $U_3(0)$ and $U_3(L)$ by multiplying the equation for u_3 by 1 and then by $(x - L/2)$ and integrating the resulting expressions. Since $\int_0^L u_{3xx}\, dx = 0$, we have $u_{3x}(L) = u_{3x}(0)$, which yields

$$U_3(L) + U_3(0) = -L\,(I_R + I_L)\,, \qquad \text{where} \qquad I_R \equiv \int_0^\infty w V_{3R}\, dy\,, \quad I_I \equiv \int_0^\infty w V_{3L}\, dy\,. \tag{4.33a}$$

Upon multiplying the u_3 equation in (4.32) by $(x - L/2)$ and integrating by parts we obtain

$$\int_0^L \left(x - \frac{L}{2} \right) u_{3xx}\, dx = \left(x - \frac{L}{2} \right) u_{3x}|_0^L - [U_3(L) - U_3(0)] = \tau_0 A' b \int_0^L \left(x - \frac{L}{2} \right)^2 dx = \frac{\tau_0 b L^3}{12} A'\,.$$

Then, by using (4.32) for $u_{3x}(0)$ and $u_{3x}(L)$ in this expression, we obtain after some algebra that

$$U_3(0) - U_3(L) = \frac{L}{2}\,(I_R - I_L) - \frac{kL^2 U_0}{2} A - \frac{b^2 L^2}{4} A^3 + \frac{\tau_0 b L^3}{24} A'\,. \tag{4.33b}$$

The linear system (4.33) for $U_3(0)$ and $U_3(L)$ is readily solved to obtain

$$\begin{pmatrix} U_3(0) \\ U_3(L) \end{pmatrix} = -\frac{L}{4} \mathcal{B} \begin{pmatrix} I_L \\ I_R \end{pmatrix} + \frac{1}{2} \left[-\frac{kL^2 U_0}{2} A - \frac{b^2 L^2}{4} A^3 + \frac{\tau_0 b L^3}{24} A' \right] \begin{pmatrix} 1 \\ -1 \end{pmatrix}; \qquad \mathcal{B} \equiv \begin{pmatrix} 3 & 1 \\ 1 & 3 \end{pmatrix}. \tag{4.34}$$

Upon substituting (4.34) into (4.30) we obtain a vector-valued NLEP for $\mathbf{V}_3 \equiv (V_{3L}, V_{3R})^T$:

$$L_0 \mathbf{V}_3 - \frac{w^2}{2} \frac{\int_0^\infty w \mathcal{B} \mathbf{V}_3\, dy}{\int_0^\infty w^2\, dy} = \left[-\frac{kLU_0}{2b} A w^2 - \frac{bL}{4} A^3 w^2 - \frac{\tau_0 L^2}{24} A' w^2 + A' w \right] \begin{pmatrix} 1 \\ -1 \end{pmatrix}. \tag{4.35}$$

Next, we diagonalize $\mathcal{B}$ and introduce a new variable $\mathbf{\Psi}$ by

$$\mathcal{B} = \mathcal{Q} \Lambda \mathcal{Q}^{-1}\,, \quad \mathcal{Q} \equiv \begin{pmatrix} 1 & 1 \\ 1 & -1 \end{pmatrix}, \quad \Lambda \equiv \begin{pmatrix} 4 & 0 \\ 0 & 2 \end{pmatrix}, \quad \mathbf{\Psi} \equiv \mathcal{Q}^{-1} \mathbf{V}_3 = \frac{1}{2} \begin{pmatrix} V_{3R} + V_{3L} \\ V_{3L} - V_{3R} \end{pmatrix}, \tag{4.36}$$

so that in terms of $\mathbf{\Psi} \equiv (\Psi_1, \Psi_2)^T$, with $\mathbf{\Psi}'(0) = 0$ and $\mathbf{\Psi} \to 0$ as $y \to +\infty$, (4.35) becomes

$$L_0 \mathbf{\Psi} - \frac{w^2}{2} \Lambda \frac{\int_0^\infty w \mathbf{\Psi}\, dy}{\int_0^\infty w^2\, dy} = \mathcal{R} \begin{pmatrix} 0 \\ 1 \end{pmatrix}, \qquad \mathcal{R} \equiv -\frac{kLU_0}{2b} A w^2 - \frac{bL}{4} A^3 w^2 - \frac{\tau_0 L^2}{24} A' w^2 + A' w\,. \tag{4.37}$$

We conclude from the two components in (4.37) that

$$L_0 \Psi_1 - 2w^2 \frac{\int_0^\infty w \Psi_1\, dy}{\int_0^\infty w^2\, dy} = 0\,, \qquad \mathcal{L} \Psi_2 \equiv L_0 \Psi_2 - w^2 \frac{\int_0^\infty w \Psi_2\, dy}{\int_0^\infty w^2\, dy} = \mathcal{R}\,. \tag{4.38}$$

As for (3.31) in §3 we conclude that $\Psi_1 \equiv 0$. Proceeding as in (3.33) of §3, the solvability condition for the second component is that $\int_0^\infty \Psi_c^\star \mathcal{R}\, dy = 0$ where $\Psi_c^\star \equiv w + yw'/2$ is the nontrivial solution to the homogeneous adjoint problem $\mathcal{L}^\star \Psi^\star = 0$. By using the integral ratio (3.35), this condition provides an explicit amplitude equation for $A(T)$. We summarize this main result as follows:

PROPOSITION 2. *Consider a small amplitude perturbation of a symmetric two-boundary spike steady-state solution of* (1.2) *when* $\mu = \mu_c - k\sigma^2$, *where* $k = \pm 1$ *and* $\mu_c = \sqrt{8b/L^3}$ *and when* $\tau_0 < \tau_{H+}(\mu_c) \approx 0.906$. *In the* $\mathcal{O}(\varepsilon)$ *boundary layers near* $x = 0$ *and* $x = L$, *we have for* $\sigma \ll 1$ *that*

(4.39)
$$\begin{aligned} &v \sim w\left[\frac{1}{U_0} + \sigma A(T) + \mathcal{O}(\sigma^2)\right], \qquad u \sim U_0 - \sigma[A(T)]^2 U_0 + \mathcal{O}(\sigma^2), \qquad \textit{(left boundary layer)},\\ &v \sim w\left[\frac{1}{U_0} - \sigma A(T) + \mathcal{O}(\sigma^2)\right], \qquad u \sim U_0 + \sigma[A(T)]^2 U_0 + \mathcal{O}(\sigma^2), \qquad \textit{(right boundary layer)}, \end{aligned}$$

where $U_0 = \sqrt{bL/2}$. *The amplitude equation for* $A(T)$ *is*

$$\frac{dA}{dT} = \frac{\theta_2}{\theta_1} A + \frac{\theta_3}{\theta_1} A^3, \qquad \textit{where} \quad \theta_1 \equiv 1 - \frac{\tau_0 L^2}{18}, \quad \theta_2 \equiv \frac{kL}{3}\sqrt{\frac{2L}{b}}, \quad \theta_3 \equiv \frac{Lb}{3} > 0, \tag{4.40}$$

where $T = \sigma^2 t$, $k = \pm 1$, *and* $b = \int_0^\infty w^2\, dy = 3$. *Since the nontrivial steady-state of* (4.40) *exists only when* $k = -1$, *for which* $\mu = \mu_c + \sigma^2$, *we conclude that the competition instability associated with the zero-eigenvalue crossing of the anti-phase mode of the linearization of the symmetric two-boundary steady-state is subcritical.*

On the range $\tau_0 < \tau_{H+}(\mu_c) < \tau_{H-}(\mu_c)$, we have $\theta_1 > 0$, with $\theta_1 = 0$ when $\tau_0 = \tau_{H-}(\mu_c) = 18/L^2$. As shown in (C.2) of Appendix C, the growth rate θ_2/θ_1 for the steady-state $A_e = 0$ of the amplitude equation (4.40) agrees with that obtained by calculating the near-zero eigenvalue of the NLEP (4.11) for the anti-phase mode when $\mu = \mu_c - \sigma^2$. From (4.40), the steady-state $A_e = 0$ is unstable when $\mu = \mu_c - \sigma^2$ ($k = 1$). On the range $\mu = \mu_c + \sigma^2$ ($k = -1$) where $A_e = 0$ is linearly stable, $A_{e\pm} = \pm\sqrt{\theta_2/\theta_3}$ are unstable equilibria of (4.40). From (4.39) the local behavior, near the bifurcation point, of the asymmetric two-boundary spike steady-state solution in the boundary layers is given by

(4.41)
$$u_e \sim U_0\left[1 \pm \left(\frac{L^3}{2b}\right)^{1/4}\sqrt{\mu - \mu_c}\right], \text{ (left layer)}; \quad u_e \sim U_0\left[1 \mp \left(\frac{L^3}{2b}\right)^{1/4}\sqrt{\mu - \mu_c}\right], \text{ (right layer)},$$

where $U_0 = \sqrt{bL/2}$ and $\mu - \mu_c = \sigma^2 \ll 1$. This weakly nonlinear analysis establishes that the competition instability at $\mu = \mu_c$ for a symmetric two-boundary spike steady-state is subcritical.

4.3. Asymmetric Boundary Spike Equilibria. Here we construct global branches of asymmetric two-boundary spike steady-state solutions of (1.2) for $\varepsilon \ll 1$. We verify that these solutions bifurcate from the symmetric two-boundary spike branch at $\mu = \mu_c$ and have the local behavior near the bifurcation point as given by the weakly nonlinear theory in (4.41).

In the left boundary layer near $x = 0$ we have $v \sim w/U_L$ and $u = U_L + \mathcal{O}(\varepsilon)$, while in the right boundary layer near $x = L$, we have $v \sim w/U_R$ and $u = U_R + \mathcal{O}(\varepsilon)$. By proceeding as in the asymptotic construction of the symmetric two-boundary spike equilibria in the beginning of §4, we obtain in the outer region that

$$u_{xx} = -\mu, \quad 0 < x < L; \qquad u_x(0^+) = b/U_L, \quad u_x(L^-) = -b/U_R, \tag{4.42}$$

where $b \equiv \int_0^\infty w^2\, dy$, $u(0^+) = U_L$, and $u(L^-) = U_R$. The explicit solution to (3.41) satisfying $u(0) = U_L$ and $u_x(0) = b/U_L$ is

$$u(x) = -\frac{\mu x^2}{2} + \frac{b}{U_L} x + U_L. \tag{4.43}$$

Then, by satisfying $u(L) = U_R$ and $u_x(L) = -b/U_R$, we obtain that U_R and U_L satisfy

$$\frac{1}{U_R} + \frac{1}{U_L} = \frac{\mu L}{b}\,, \qquad (U_R - U_L)\left(1 - \frac{bL}{2U_L U_R}\right) = 0\,. \tag{4.44}$$

The symmetric two-boundary spike solution is obtained by setting $U_R = U_L$, which yields

$$U_L = U_R = \frac{2b}{\mu L}\,, \qquad b \equiv \int_0^\infty w^2\,dy = 3\,. \tag{4.45}$$

In contrast, for the asymmetric solutions where $U_L \neq U_R$, we obtain from (4.44) that $U_L U_R = bL/2$ and that U_L and U_R are the two roots of the quadratic equation $U^2 - \mu L^2 U/2 + bL/2 = 0$. This yields

$$U_L = \frac{\mu L^2}{4}\left[1 \pm \sqrt{1 - \left(\frac{\mu_c}{\mu}\right)^2}\,\right], \quad U_R = \frac{\mu L^2}{4}\left[1 \mp \sqrt{1 - \left(\frac{\mu_c}{\mu}\right)^2}\,\right], \qquad \text{where} \quad \mu_c \equiv \sqrt{\frac{8b}{L^3}}\,, \tag{4.46}$$

provided that $\mu > \mu_c$. As $\mu \to \mu_c$ from above, a Taylor series approximation of (4.46) yields that

$$U_L \sim \sqrt{\frac{bL}{2}}\left[1 \pm \left(\frac{L^3}{2b}\right)^{1/4}\sqrt{\mu - \mu_c}\,\right], \quad U_R \sim \sqrt{\frac{bL}{2}}\left[1 \mp \left(\frac{L^3}{2b}\right)^{1/4}\sqrt{\mu - \mu_c}\,\right], \quad \text{as} \quad \mu \to \mu_c\,. \tag{4.47}$$

This expression agrees with the result given in (4.41) from the amplitude equation.

In the right panel of Fig. 7 we use (4.46) to plot global branches of asymmetric two-boundary spike equilibria versus μ when $L = 2$. In this figure the symmetric branch is given by (4.45), while the dashed-dotted curves are the steady-state results (4.47) from the amplitude equation, as obtained from the weakly nonlinear theory in §4.2. In the left panel of Fig. 7 we plot an asymmetric two-boundary spike solution when $\mu = 2.0$ and $L = 2$.

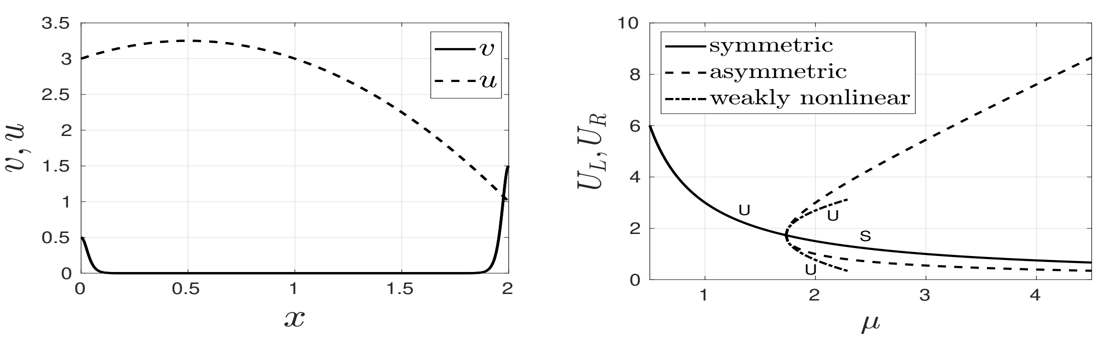

FIG. 7. *Left panel: The asymmetric two-boundary spike solution for $L = 2$, $\varepsilon = 0.02$, and $\mu = 2.0$ with u as given in (4.43) and $v \sim w(\varepsilon^{-1}x)/U_L + w(\varepsilon^{-1}(L - x))/U_R$, where $w(y)$ is the homoclinic in (2.3). Right panel: Global branches of asymmetric and symmetric two-boundary spike equilibria obtained from (4.46) and (4.45), respectively, together with the local behavior in (4.47) predicted from the weakly nonlinear theory for $L = 2$ and $\varepsilon = 0.02$. Linear stability results are indicated.*

In Fig. 8 we show a favorable comparison between the asymptotic result (4.47) obtained from the weakly nonlinear theory with corresponding full numerical results computed using COCO [4] for branches of symmetric and asymmetric two-boundary spike equilibria for the steady-state of the Schnakenberg model (1.2). The comparison is shown near the symmetry-breaking bifurcation point $\mu = \mu_c$ when $L = 2$ and $\varepsilon = 0.01$.

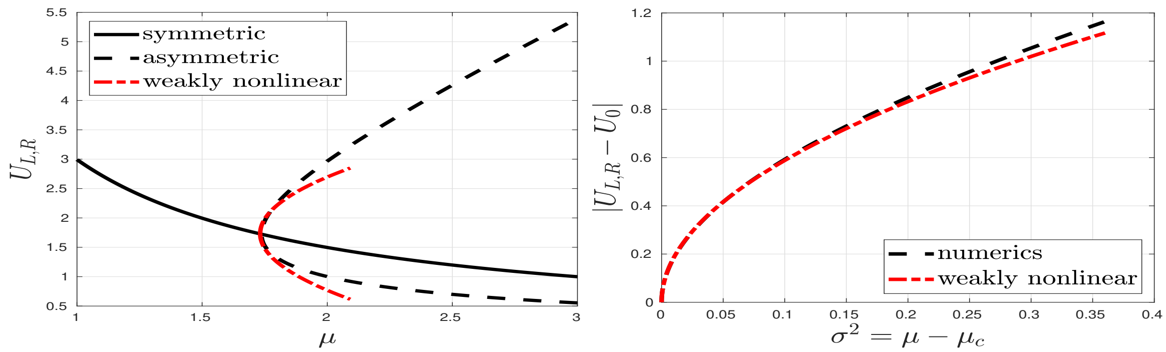

FIG. 8. *Left panel: Numerical bifurcation branches of symmetric (full black curve) and asymmetric (dashed black curve) two-boundary spike equilibria for the Schnakenberg model versus μ, as computed with* COCO *[4] upon discretizing the steady-state of the PDE system (1.2) with $N = 800$ mesh points. The dot-dashed red curve is the weakly nonlinear prediction (4.47) for the asymmetric pattern. Parameters are $L = 2$ and $\varepsilon = 0.01$. Right panel: A zoomed-in view of the amplitude of the asymmetric equilibria shifted to the origin.*

5. Generalized GM Model: Asymmetric Boundary Spike Equilibria. In this section we consider the generalized GM model on $0 \leq x \leq L$ with exponent set (p, q, m, s), formulated as

$$v_t = \varepsilon^2 v_{xx} - v + \frac{v^p}{u^q}\,, \qquad \tau_0 u_t = u_{xx} - \mu u + \varepsilon^{-1}\frac{v^m}{u^s}\,, \tag{5.1}$$

with $v_x = u_x = 0$ at $x = 0, L$. Here $\varepsilon \ll 1$, $\mu = \mathcal{O}(1)$ and $\tau_0 = \mathcal{O}(1)$ are positive constants, and the exponent set satisfies $p > 1$, $q > 0$, $m > 1$, $s \geq 0$, with $\xi \equiv mq/(p-1) - (s+1) > 0$.

An NLEP linear stability theory can be used to show that symmetric two-boundary spike equilibria for this general GM model are linearly stable only on the range $\mu > \mu_c$ when τ_0 is below some threshold. This competition instability threshold μ_c obtained from NLEP theory is the symmetry-breaking bifurcation value for the emergence of asymmetric two-boundary spike equilibria, and is given in (5.6) below. For $\mu < \mu_c$, symmetric two-boundary spike equilibria are unstable for any $\tau_0 \geq 0$. To determine whether the competition instability is subcritical, as for the case of the prototypical exponent set $(p, q, m, s) = (2, 1, 2, 0)$, we will proceed to derive and analyze a nonlinear algebraic system characterizing asymmetric two-boundary spike equilibria for (5.1). By plotting such global branches of equilibria and analytically characterizing their local branching behavior near the symmetry-breaking bifurcation point, we will infer that a competition instability of symmetric two-boundary spike equilibria is always subcritical for the general GM model (5.1). This simple approach allows us to infer subcriticality of the competition instability without having to directly derive an amplitude equation based on retaining weakly nonlinear terms beyond the linearized NLEP theory. Such a derivation of an amplitude equation for this generalized GM model (5.1) is rather intractable analytically.

The matched asymptotic analysis approach to calculate asymmetric two-boundary spike equilibria for (5.1) is similar to that described in §3.2, and so we only outline the analysis. In the left boundary layer near $x = 0$ we have $v \sim U_L^{q/(p-1)} w$ and $u = U_L + \mathcal{O}(\varepsilon)$, while in the right boundary layer near $x = L$, we have $v \sim U_R^{q/(p-1)} w$ and $u = U_R + \mathcal{O}(\varepsilon)$. Here $w(y)$ is the unique homoclinic solution to $w'' - w + w^p = 0$, which is given explicitly by

$$w(y) = \left[\left(\frac{p+1}{2}\right)\operatorname{sech}^2\left(\frac{(p-1)}{2}y\right)\right]^{1/(p-1)}. \tag{5.2}$$

By matching the boundary layer solutions for u to the outer solution, we obtain in the outer region that the leading-order inhibitor field satisfies

$$u_{xx} - \mu u = 0\,, \quad 0 < x < L\,; \qquad u_x(0^+) = -U_L^{\xi+1} b_m\,, \quad u_x(L^-) = U_R^{\xi+1} b_m\,, \tag{5.3}$$

where $b_m \equiv \int_0^\infty w^m \, dy$, $u(0^+) = U_L$ and $u(L^-) = U_R$. The explicit solution to (5.3) is (3.42) and, by satisfying the flux boundary conditions at the endpoints, we obtain the nonlinear algebraic system

$$\text{(5.4a)} \quad \begin{pmatrix} z_L^{\xi+1} \\ z_R^{\xi+1} \end{pmatrix} = \mathcal{A} \begin{pmatrix} z_L \\ z_R \end{pmatrix}; \qquad \mathcal{A} \equiv \begin{pmatrix} \coth(\sqrt{\mu}L) & -\operatorname{csch}(\sqrt{\mu}L) \\ -\operatorname{csch}(\sqrt{\mu}L) & \coth(\sqrt{\mu}L) \end{pmatrix}, \quad \xi \equiv \frac{mq}{p-1} - (s+1),$$

where z_L and z_R are related to U_L and U_R by

$$\text{(5.4b)} \qquad U_L = \left(\frac{\sqrt{\mu}}{b_m}\right)^{1/\xi} z_L, \qquad U_R = \left(\frac{\sqrt{\mu}}{b_m}\right)^{1/\xi} z_R.$$

Symmetric two-boundary spike equilibria are obtained by setting $\mathbf{z} \equiv (z_L, z_R)^T = z_c \mathbf{e}$, where $\mathbf{e} \equiv (1,1)^T$. Upon using $\mathcal{A}\mathbf{e} = \tanh\left(\sqrt{\mu}L/2\right)\mathbf{e}$, we obtain

$$\text{(5.5)} \qquad U_L = U_R = \left(\frac{\sqrt{\mu}}{b}\right)^{1/\xi} z_c, \qquad \text{where} \qquad z_c = \left[\tanh\left(\frac{\sqrt{\mu}L}{2}\right)\right]^{1/\xi}.$$

To determine the bifurcation point along the symmetric branch where asymmetric equilibra emerge, we linearize (5.4a) about $\mathbf{z} = z_c\mathbf{e}$ by writing $\mathbf{z} = z_c\mathbf{e} + \eta$, where $|\eta| \ll 1$. This yields the linearized problem $\mathcal{A}\eta = (\xi+1) z_c^{\xi} \eta$. Since $\mathcal{A}\mathbf{q} = \coth\left(\sqrt{\mu}L/2\right)\mathbf{q}$, where $\mathbf{q} = (1,-1)^T$, we conclude that $\eta = (1,-1)^T$ is a nontrivial solution to the linearized problem provided that $(\xi+1)z_c^{\xi} = \coth\left(\sqrt{\mu}L/2\right)$. Using (5.5) for z_c^{ξ}, we conclude that the symmetry-breaking bifurcation value $\mu = \mu_c$ occurs when

$$\text{(5.6)} \qquad \tanh\left(\frac{\sqrt{\mu}L}{2}\right) = \sqrt{\frac{1}{\xi+1}}, \qquad \text{so that} \qquad \mu_c = \frac{4}{L^2}\left[\ln\left(\frac{1}{\sqrt{\xi}} + \sqrt{\frac{1}{\xi}+1}\right)\right]^2.$$

Observe that when $(p,q,m,s) = (2,1,2,0)$, for which $\xi = 1$, μ_c in (5.6) reduces to that given in (2.17).

To obtain global branches of asymmetric two-boundary spike equilibria we rewrite (5.4a) as

$$\text{(5.7)} \qquad z_L^{\xi+1} + z_R^{\xi+1} = \tanh\left(\frac{\sqrt{\mu}L}{2}\right)(z_L + z_R), \qquad z_L^{\xi+1} - z_R^{\xi+1} = \coth\left(\frac{\sqrt{\mu}L}{2}\right)(z_L - z_R).$$

Next, we define $\omega \equiv z_L/z_R$, and from (5.7) we readily obtain the following parameterization of asymmetric two-boundary spike equilibria in terms of ω:

$$\text{(5.8)} \qquad \begin{aligned} z_R &= \left(\frac{1}{2\omega^{\xi+1}}\left[\sqrt{R(\omega)}(\omega+1) + \frac{1}{\sqrt{R(\omega)}}(\omega-1)\right]\right)^{1/\xi}, \qquad z_L = \omega z_R, \\ \mu &= \frac{4}{L^2}\left[\ln\left(\frac{1+\sqrt{R(\omega)}}{\sqrt{1-R(\omega)}}\right)\right]^2, \qquad \text{where} \qquad R(\omega) \equiv \frac{(\omega-1)}{(\omega^{\xi+1}-1)}\frac{(\omega^{\xi+1}+1)}{(\omega+1)}. \end{aligned}$$

In terms of the parameter $\omega > 0$, the parameterization (5.8) together with (5.4b) determines the global bifurcation diagram of U_L and U_R in terms of μ for asymmetric two-boundary spike equilibria of (5.1) without the need for having to numerically solve any nonlinear algebraic system.

The symmetry-breaking bifurcation point occurs when $\omega \to 1$. Using L'hopital's rule we obtain $R(1) = 1/(\xi+1)$, which recovers $\mu = \mu_c$ from (5.8) and (5.6). To determine the local branching behavior of asymmetric two-boundary spike equilibria we first use Taylor series on (5.8) to get

$$\text{(5.9)} \qquad R(\omega) \sim \frac{1}{(\xi+1)}\left[1 + \frac{1}{12}(\xi^2+2\xi)(\omega-1)^2 + \ldots\right], \quad \text{as} \quad \omega \to 1.$$

Then, we relate $\mu - \mu_c$ to $\omega - 1$ by using $\tanh\left(\sqrt{\mu}L/2\right) = [R(\omega)]^{1/2}$, which yields

$$(\omega-1)^2 \sim \frac{6L}{(\xi+2)\sqrt{\mu_c(\xi+1)}}(\mu-\mu_c)\,, \quad \text{as} \quad \mu \to \mu_c^+\,. \tag{5.10}$$

From this key expression we observe that asymmetric two-boundary spike equilibria exist near the bifurcation point only in the subcritical range where $\mu > \mu_c$.

Next, we calculate z_R as $\omega \to 1$. Since $R(\omega) \sim 1/(\xi+1) + \mathcal{O}((\omega-1)^2)$ as $\omega \to 1$, we calculate

$$\sqrt{R(\omega)}(\omega+1) + \frac{1}{\sqrt{R(\omega)}}(\omega-1) \sim 2\sqrt{R(1)}\left[1 + \frac{(\omega-1)}{2}\left(1 + \frac{1}{R(1)}\right) + \mathcal{O}((\omega-1)^2)\right].$$

By using this expression to estimate $z_R(\omega)$ in (5.8) we get

$$\begin{aligned} z_R(\omega) &\sim \left(\sqrt{R(1)}\right)^{1/\xi}(1+(\omega-1))^{-1-1/\xi}\left(1+\frac{(\xi+2)}{2}(\omega-1)\right)^{1/\xi} + \mathcal{O}((\omega-1)^2)\,,\\ &\sim \left(\sqrt{R(1)}\right)^{1/\xi}\left(1-\frac{(\xi+1)}{\xi}(\omega-1)\right)\left(1+\frac{(\xi+2)}{2\xi}(\omega-1)\right) + \mathcal{O}((\omega-1)^2)\,,\\ &\sim \left(\sqrt{R(1)}\right)^{1/\xi}\left(1-\frac{1}{2}(\omega-1)\right) + \mathcal{O}((\omega-1)^2)\,. \end{aligned} \tag{5.11}$$

By using this expression in (5.4b), and recalling that $R(1) = 1/(\xi+1)$, we get

$$U_R \sim \left(\frac{\sqrt{\mu}}{b_m\sqrt{\xi+1}}\right)^{1/\xi}\left(1 - \frac{1}{2}(\omega-1) + \mathcal{O}((\omega-1)^2)\right). \tag{5.12}$$

Finally, by using (5.10) together with $\sqrt{\mu} = \sqrt{\mu_c} + \mathcal{O}(\mu-\mu_c)$, we conclude that

$$U_R \sim \left(\frac{\sqrt{\mu_c}}{b_m\sqrt{\xi+1}}\right)^{1/\xi}\left(1 \pm \sqrt{\frac{3L}{2(\xi+2)\sqrt{\mu_c(\xi+1)}}}\sqrt{\mu-\mu_c} + \mathcal{O}(\mu-\mu_c)\right), \quad \text{as} \quad \mu\to\mu_c^+\,. \tag{5.13}$$

Here μ_c is defined in (5.6) and $b_m \equiv \int_0^\infty w^m\,dy$, where w is the homoclinic in (5.2). An identical expression holds for U_L upon replacing $\pm$ by $\mp$ in (5.13). For the prototypical GM model with exponent set $(p,q,m,s) = (2,1,2,0)$, where $\xi = 1$, we obtain that (5.13) reduces to that in (3.47).

For the exponent sets $(p,q,m,s) = (2,1,3,0)$ and $(p,q,m,s) = (4,2,2,0)$, in the left and right panels of Fig. 9, respectively, we plot global branches of asymmetric two-boundary spike equilibria versus μ as obtained from (5.8) and (5.4b) when $L = 2$. The symmetric branch, as given in (5.5), is also shown. The dashed-dotted curves in these figures are the local results (5.13), valid near the symmetry-breaking bifurcation point, characterizing the local behavior of the subcritical bifurcation.

6. Discussion. Competition, or overcrowding, instabilities of localized 1-D spike patterns for singularly perturbed RD systems have previously been implicated through full PDE simulations of playing a central role in triggering spike annihilation events, which results in a rather intricate coarsening process of a multi-spike pattern (cf. [1], [14], [22], [29]). Qualitatively, a competition instability for a spike pattern for the 1-D GM model, which has the effect of locally preserving the sum of the heights of the spikes, occurs when either the inhibitor decay rate is slowly ramped below a critical value or, equivalently, when the inter-spike distance falls below a threshold. For the 1-D Schnakenberg model, a competition instability will occur when the feed-rate parameter in (1.2) decreases below some critical value. Although explicit criteria on the parameters in the 1-D GM and Schnakenberg models for the onset of this linear instability can be calculated by analyzing the spectrum of the NLEP of

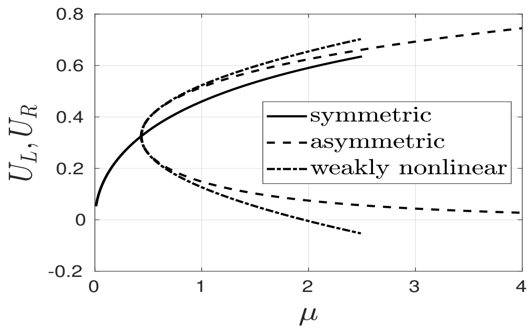

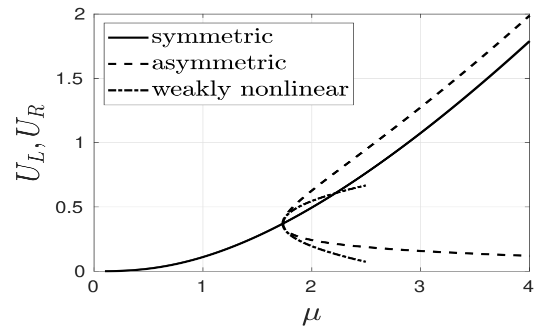

FIG. 9. *Global branches of asymmetric and symmetric two-boundary spike equilibria for the generalized GM model* (5.1) *as obtained from from* (5.8) *(with* (5.4b)*) and* (5.5)*, respectively. The dashed-dotted curves are the local branching behavior* (5.13) *near the symmetry-breaking bifurcation point. The domain length is $L = 2$. Left figure: exponent set $(p, q, m, s) = (2, 1, 3, 0)$. Right figure: exponent set $(p, q, m, s) = (4, 2, 2, 0)$.*

the linearization, it has been an open problem to develop a weakly nonlinear theory to establish that a competition instability is subcritical.

For the 1-D GM and Schnakenberg models we have developed and implemented a weakly nonlinear theory to show analytically that a competition instability for a symmetric two-boundary spike steady-state is subcritical. In this context, we have shown explicitly that the competition instability threshold corresponds to a symmetry-breaking bifurcation point where an unstable branch of asymmetric two-boundary spike equilibria emerges from the symmetric steady-state solution branch. Two boundary spikes interacting through a bulk diffusion field represents the simplest spatial configuration of interacting localized spikes that can undergo a competition instability. A competition instability can also occur for 1-D multi-spike patterns with spikes interior to the domain, and from PDE simulations this linear instability mechanism can also trigger a nonlinear process leading to spike annihilation (cf. [29], [18], [1]). The challenging feature with providing a weakly nonlinear analysis for patterns with interior spikes is that the analysis would have to couple weak spike amplitude instabilities near onset to the weak translation instabilities resulting from the slow spatial dynamics of the centers of the spikes. For our weakly nonlinear boundary spike analysis, where the spike locations are fixed at the boundaries, there was no complicating feature of having to include in the analysis any small eigenvalues associated with drift instabilities of the spike locations.

We conclude by briefly remarking on two possible extensions of this study. One open problem is to determine whether there are specific singularly perturbed RD systems for which competition instabilities are supercritical and not subcritical. One simple method to try to identify such an RD system consists of extending the approach used in §5 for constructing asymmetric two-boundary spike equilibria of the generalized GM model (5.1) to a general class of singularly perturbed RD system. For an RD system where the competition instability is supercritical, in the bifurcation diagram of two-boundary spike equilibria there should exist a branch of asymmetric equilibria on the parameter range where the symmetric steady-state branch is linearly unstable. In [16], it was shown for a GM model with a spatially variable precursor field that linear stable asymmetric equilibria with two-interior spikes can occur for a certain parameter range. However, it is an open problem to determine if one construct linearly stable asymmetric spike equilibria for an RD system without the spatial gradient in the reaction-kinetics. Finally, a second open direction is to extend the weakly nonlinear analysis of competition instabilities of 1-D spike patterns to the 2-D context of localized spot patterns near parameter values where the 2-D NLEP associated with the linearization has a zero-eigenvalue crossing.

7. Acknowledgements. Theodore Kolokolnikov and Michael Ward were supported by NSERC Discovery grants. Frédéric Paquin-Lefebvre was supported by a UBC Four-Year Graduate Fellowship.

Appendix A. Numerical Computation of Hopf Bifurcation Thresholds: GM Model. We outline the approach used to compute Hopf bifurcation thresholds for (2.16). From (2.16a) we have $\Phi = \chi_{\pm}(L_0-\lambda)^{-1}w^2 \int_0^\infty w\Phi\, dy / \int_0^\infty w^2\, dy$. Upon multiplying by w and integrating we get

$$\int_0^\infty w\Phi\, dy \left[\frac{1}{\chi_{\pm}} - \frac{\int_0^\infty w(L_0-\lambda)^{-1}w^2\, dy}{\int_0^\infty w^2\, dy} \right] = 0\,.$$

Any unstable eigenvalue of the NLEP (2.16) must be such that $\int_0^\infty w\Phi\, dy \neq 0$. As such, discrete eigenvalues of the NLEP are roots of $g_{\pm}(\lambda)=0$, where

$$g_{\pm}(\lambda) \equiv \frac{1}{\chi_{\pm}(\lambda,\mu)} - \mathcal{F}(\lambda)\,, \qquad \text{where} \qquad \mathcal{F}(\lambda) \equiv \frac{\int_0^\infty w(L_0-\lambda)^{-1}w^2\, dy}{\int_0^\infty w^2\, dy}\,. \tag{A.1}$$

Here $\chi_{\pm}(\lambda,\mu)$ for the in-phase $(+)$ and anti-phase modes $(-)$ are defined in (2.16b). The competition instability threshold, obtained from the anti-phase mode, is found by setting $g_{-}(0)=0$. Since $\mathcal{F}(0)=1$, this occurs when $\chi_{-}(0,\mu)=1$, which yields $\mu=\mu_c$ where $\sqrt{\mu_c}L = 2\ln(1+\sqrt{2})$.

To determine the Hopf bifurcation thresholds for a given domain length L we set $\lambda = i\lambda_I$, with $\lambda_I>0$, and use Newton's method on $g_{\pm}(i\lambda_I)=0$ to compute $\tau_{H\pm}=\tau_{H\pm}(\mu)$ and $\lambda_{IH\pm}=\lambda_{IH\pm}(\mu)$. The results were shown in Fig. 3 when $L=2$. For the anti-phase mode, a Hopf threshold exists only when $\mu>\mu_c$, and $\lambda_{IH-}\to 0$ as $\mu\to\mu_c$ from above. To determine the Hopf threshold value of τ_{H-} at $\mu=\mu_c$, we set $\mu=\mu_c$ and use a perturbation approach to estimate $\mathrm{Im}\,(g_{-}(i\lambda_I)) \sim a_c\lambda_I + \mathcal{O}(\lambda_I^3)$ as $\lambda_I\to 0$. By setting $a_c=0$, we obtain τ_{H-}.

To this end, we set $\mathrm{Im}(g_{-}(i\lambda_I))=0$ to obtain, upon using the explicit expression for χ_{-} in (2.16b), together with $\tanh\left(\sqrt{\mu_c}L/2\right) = 1/\sqrt{2}$, that

$$\mathrm{Im}(g_{-}(i\lambda_I)) = \mathrm{Im}\left[\frac{\sqrt{1+iz}}{\sqrt{2}} \coth\left(\beta\sqrt{1+iz}\right) - \mathcal{F}(i\lambda_I) \right]\,, \tag{A.2}$$

where we have defined $z\equiv \tau_{H-}\lambda_I/\mu$ and $\beta\equiv\sqrt{\mu_c}L/2$. For $\lambda_I\to 0$ we use $\sqrt{1+z}\sim 1+z/2$, $\coth(\beta+\beta z/2)\sim\coth(\beta) - \frac{\beta z}{2}\mathrm{csch}^2(\beta)$ for $z\ll 1$, together with $\coth(\beta)=\sqrt{2}$ and $\mathrm{csch}(\beta)=1$. Moreover, we have $\mathrm{Im}\left(\mathcal{F}(i\lambda_I)\right)\sim 3\lambda_I/4$ from Proposition 3.2 of [29]. In this way, and upon recalling $\sqrt{\mu_c}L = 2\ln(1+\sqrt{2})$, we obtain from (A.2) that as $\lambda_I\to 0$,

$$\mathrm{Im}(g_{-}(i\lambda_I)) \sim a_c\lambda_I + \mathcal{O}(\lambda_I^3)\,, \quad \text{where} \quad a_c \equiv \frac{\tau_{H-}}{2\sqrt{2}\mu_c}\left(\sqrt{2} - \ln(1+\sqrt{2})\right) - \frac{3}{4}\,. \tag{A.3}$$

Upon setting $a_c=0$, we obtain the explicit expression for τ_{H-} as given in (2.19).

Appendix B. Perturbation of Linear Instability Threshold: GM Model. In this appendix we verify the expression for the coefficient θ_2/θ_1 of A in the amplitude equation (3.39a) by setting $\mu=\mu_c-\sigma^2$ and calculating for $\sigma\ll 1$ the near-zero eigenvalue for

$$L_0\Phi - \chi_{-}(\lambda,\mu)w^2\left(\frac{\int_0^\infty w\Phi\, dy}{\int_0^\infty w^2\, dy} \right) = \lambda\Phi\,; \qquad \chi_{-}(\lambda,\mu) = \frac{2\sqrt{\mu}}{\sqrt{\mu+\tau_0\lambda}} \frac{\tanh\left(\sqrt{\mu}L/2\right)}{\coth\left(\theta_\lambda L/2\right)}\,, \tag{B.1}$$

with $\theta_\lambda = \sqrt{\mu+\tau_0\lambda}$, for which $\Phi_y(0)=0$ and $\lim_{y\to\infty}\Phi(y)=0$. Since $\chi_{-}(0,\mu_c)=1$ and $L_0 w = w^2$, we expand the critical eigenpair as

$$\lambda = \sigma^2\lambda_1 + \ldots\,, \qquad \Phi = w + \sigma^2\Phi_1 + \ldots\,, \qquad \text{when} \qquad \mu = \mu_c - \sigma^2\,. \tag{B.2}$$

Upon substituting (B.2) into (B.1), we collect powers of σ^2 to obtain that

$$\text{(B.3)}\qquad \mathcal{L}\Phi_1 \equiv L_0\Phi_1 - w^2\left(\frac{\int_0^\infty w\Phi_1\,dy}{\int_0^\infty w^2\,dy}\right) = \mathcal{R} \equiv \lambda_1 w - \partial_\mu\chi_-(0,\mu_c)w^2 + \lambda_1 w^2\partial_\lambda\chi_-(0,\mu_c)\,.$$

Since the homogeneous adjoint problem $\mathcal{L}^\star\Psi^\star = 0$ has the nontrivial solution $\Psi^\star = \Psi_c^\star \equiv w + yw'/2$ (see (3.33b)), the solvability condition $\int_0^\infty \Psi_c^\star\mathcal{R}\,dy = 0$ for (B.3) yields that

$$\text{(B.4)}\qquad \lambda_1 = \left[\lambda_1\partial_\lambda\chi_-(0,\mu_c) + \partial_\mu\chi_-(0,\mu_c)\right]J\,,\qquad \text{where}\qquad J \equiv \frac{\int_0^\infty w^2\Psi_c^\star\,dy}{\int_0^\infty w\Psi_c^\star\,dy}\,.$$

Since $J = 4/3$, as calculated in (3.35), we get

$$\text{(B.5)}\qquad \lambda_1\left(1 - \frac{4}{3}\partial_\lambda\chi_-(0,\mu_c)\right) = \frac{4}{3}\partial_\mu\chi_-(0,\mu_c)\,.$$

By using (B.1) for $\chi_-(\lambda,\mu)$, we evaluate the required partial derivatives and use $\sinh\left(\sqrt{\mu_c}L/2\right) = 1$ and $\cosh\left(\sqrt{\mu_c}L/2\right) = \sqrt{2}$ to simplify the resulting expressions. In this way, we calculate that

$$\text{(B.6)}\qquad \begin{aligned} \partial_\mu\chi_-(0,\mu_c) &= \frac{L}{\sqrt{\mu_c}}\operatorname{sech}^2\left(\frac{\sqrt{\mu_c}L}{2}\right)\tanh\left(\frac{\sqrt{\mu_c}L}{2}\right) = \frac{\sqrt{2}L}{4\sqrt{\mu_c}}\,,\\ \partial_\lambda\chi_-(0,\mu_c) &= -\frac{\tau_0}{\mu_c}\tanh^2\left(\frac{\sqrt{\mu_c}L}{2}\right) + \frac{\tau_0 L}{2\sqrt{\mu_c}}\tanh\left(\frac{\sqrt{\mu_c}L}{2}\right)\operatorname{sech}^2\left(\frac{\sqrt{\mu_c}L}{2}\right)\\ &= \frac{\tau_0}{2\mu_c}\left(-1 + \frac{L\sqrt{2\mu_c}}{4}\right)\,. \end{aligned}$$

Finally, by substituting (B.6) into (B.5), and by recalling $\sqrt{\mu_c}L = 2\ln(1+\sqrt{2})$, we conclude that

$$\text{(B.7)}\qquad \lambda_1 = \frac{\sqrt{2}L}{3\sqrt{\mu_c}}\left[1 + \frac{2\tau_0}{3\mu_c}\left(\frac{\sqrt{2}}{2}\ln(1+\sqrt{2}) - 1\right)\right]^{-1}\,.$$

We observe, as anticipated, that this expression for λ_1 agrees with the ratio θ_2/θ_1 of the linear term in the amplitude equation (3.39a) when $k = 1$.

Appendix C. Numerical Computation of Hopf Bifurcation Thresholds: Schnakenberg.

Following the approach in Appendix A, we obtain that the discrete eigenvalues of the NLEP (4.11) for the Schnakenberg model are the roots of $g_\pm(\lambda) = 0$, where

$$\text{(C.1a)}\quad g_\pm(\lambda) \equiv \frac{1}{\chi_\pm(\lambda,\mu)} - \mathcal{F}(\lambda)\,;\qquad \frac{1}{\chi_\pm(\lambda,\mu)} = \begin{cases} \frac{1}{2}\left(1 + \left(\frac{\mu_c}{\mu}\right)^2 z\tanh(z)\right)\,, & \text{in-phase } (+)\,,\\ \frac{1}{2}\left(1 + \left(\frac{\mu_c}{\mu}\right)^2 z\coth(z)\right)\,, & \text{anti-phase } (-)\,. \end{cases}$$

Here $\mathcal{F}(\lambda)$ is defined in (A.1), while z and μ_c are defined by

$$\text{(C.1b)}\qquad z \equiv \sqrt{\hat{\tau}\lambda}\,,\qquad \hat{\tau} \equiv \frac{\tau_0 L^2}{4}\,,\qquad \mu_c \equiv \sqrt{\frac{8b}{L^3}}\,,\qquad b = \int_0^\infty w^2\,dy = 3\,.$$

The competition instability threshold, associated with the anti-phase mode, is found by setting $g_-(0) = 0$. Since $\mathcal{F}(0) = 1$ this occurs when $\chi_-(0,\mu_c) = 1$, which yields $\mu_c = \sqrt{8b/L^3}$. When $\mu < \mu_c$, the NLEP for the anti-phase mode has an unstable real positive eigenvalue.

The Hopf bifurcation thresholds for the anti-phase and in-phase modes are obtained by setting $\lambda = i\lambda_I$, with $\lambda_I > 0$, and using Newton's method on $\text{Re}\,[g_\pm(i\lambda_I)] = 0$ and $\text{Im}\,[g_\pm(i\lambda_I)] = 0$ to determine a parametric form of the Hopf threshold $\lambda_I = \lambda_{IH\pm}$ and $\hat{\tau} = \hat{\tau}_{H\pm}$ depending only on the ratio μ_c/μ. Then, the scaling law in (C.1b) gives the Hopf thresholds in terms of L as $\tau_{H\pm} = 4\hat{\tau}_{H\pm}/L^2$. The results were shown in Fig. 6 for $L = 2$. For the anti-phase mode, a Hopf threshold exists only on the range $\mu > \mu_c$, and $\lambda_{IH-} \to 0$ as $\mu \to \mu_c$ from above.

To analytically calculate the Hopf threshold value τ_{H-} for the anti-phase mode at $\mu = \mu_c$, we set $\mu = \mu_c$ and we estimate $\text{Im}\,(g_-(i\lambda_I)) \sim a_c\lambda_I + \mathcal{O}(\lambda_I^3)$ as $\lambda_I \to 0$. By setting $a_c = 0$, we obtain τ_{H-}. To this end, we use $z\coth(z) \sim 1 + z^2/3$ as $z \to 0$ together with $\text{Im}\,(\mathcal{F}(i\lambda_I)) \sim 3\lambda_I/4$ (see Proposition 3.2 of [29]) to calculate for $\lambda_I \to 0$ that $\text{Im}(g_-(i\lambda_I)) \sim a_c\lambda_I + \mathcal{O}(\lambda_I^3)$ where $a_c = \hat{\tau}/6 - 3/4$. Upon setting $a_c = 0$, and using $\hat{\tau} \equiv \tau_0 L^2/4$, we obtain $\tau_0 = \tau_{H-} = 18/L^2$ when $\mu = \mu_c$, as given in (4.12).

Finally, we verify the coefficient of A in the amplitude equation (4.40) by setting $\mu = \mu_c - \sigma^2$ and calculating for $\sigma \ll 1$ the unstable eigenvalue to the NLEP (4.11) for the anti-phase mode. Rather than working with the NLEP (4.11) directly as in Appendix B, we instead, equivalently, calculate the root to $g_-(\lambda) = 0$ on the positive real axis with $\lambda = \sigma^2\lambda_1 \ll 1$. We set $\mu = \mu_c - \sigma^2$ and calculate using $z\coth(z) \sim 1 + z^2/3 + \ldots$ with $z = \sqrt{\tau_0\lambda}L/2$ that

$$\frac{1}{\chi_-} \sim \frac{1}{2} + \frac{1}{2}\left(\frac{\mu_c}{\mu_c - \sigma^2}\right)^2 \left(1 + \frac{\tau_0 L^2}{12}\sigma^2\lambda_1 + \ldots\right) \sim 1 + \sigma^2\left(\frac{\tau_0 L^2 \lambda_1}{24} + \frac{1}{\mu_c}\right).$$

Moreover, on the real positive axis we have from Proposition 3.5 of [29] that $\mathcal{F}(\lambda) \sim 1 + 3\lambda/4$ as $\lambda \to 0$. In this way, we conclude for $\sigma \to 0$ that

$$g_-(\sigma^2\lambda_1) \sim \sigma^2\left(\frac{\tau_0 L^2}{24}\lambda_1 + \frac{1}{\mu_c} - \frac{3}{4}\lambda_1\right) + \ldots.$$

From the condition $g_-(\sigma^2\lambda_1) = 0$, and upon using $\mu_c = \sqrt{8b/L^3}$, we obtain that

$$\text{(C.2)} \qquad \lambda_1\left(1 - \frac{\tau_0 L^2}{18}\right) = \frac{4}{3\mu_c} = \frac{L}{3}\sqrt{\frac{2L}{b}}, \qquad \text{where} \qquad b = \int_0^\infty w^2\,dy = 3.$$

By comparing (C.2) with the amplitude equation (4.40) when $k = 1$, we get $\lambda_1 = \theta_2/\theta_1$ as expected.

REFERENCES

[1] R. Bastiaansen, A. Doelman, *The dynamics of disappearing pulses in a singularly perturbed reaction diffusion system with parameters that vary in space and time*, Physica D, **388**, (2019), pp. 45–72.

[2] C. N. Chen, S. I. Ei, S. Tzeng, *Heterogeneity-induced effects for pulse dynamics in Fitzhugh-Nagumo type systems*, Physica D, **382-383**(1), (2018), pp. 22–32.

[3] M. Cross, P. Hohenberg, *Pattern formation outside of equilibrium*, Rev. Mod. Physics, **65**, (1993), pp. 851-1112.

[4] H. Dankowicz, F. Schilder, *Recipes for continuation*, in the book series *Computational Sciences and Engineering*, SIAM Publications, (2013), xv + 564 pages.

[5] A. Doelman, R. A. Gardner, T. J. Kaper, *Stability analysis of singular patterns in the 1d Gray-Scott model: A matched asymptotics approach*, Physica D, **122**(1-4), (1998), pp. 1-36.

[6] A. Doelman, R. A. Gardner, T. Kaper, *Large stable pulse solutions in reaction-diffusion equations*, Indiana U. Math. J., **50**(1), (2001), pp. 443-507.

[7] A. Doelman, T. Kaper, *Semistrong pulse interactions in a class of coupled reaction-diffusion equations*, SIAM J. Appl. Dyn. Sys., **2**(1), (2003), pp. 53-96.

[8] A. Doelman, T. Kaper, K. Promislow, *Nonlinear asymptotic stability of the semi-strong pulse dynamics in a regularized Gierer-Meinhardt model*, SIAM J. Math. Anal., **38**(6), (2007), pp. 1760–1789.

[9] S. I. Ei, *The motion of weakly interacting pulses in reaction-diffusion systems*, J. Dynam. Diff. Eq., **14**, (2002), pp. 85–137.

[10] A. Gierer, H. Meinhardt, *A theory of biological pattern formation*, Kybernetik, **12**, (1972), pp. 30–39.

[11] D. Gomez, L. Mei, J. Wei, *Stable and unstable periodic spiky solutions for the Gray-Scott system and the Schnakenberg system*, to appear, J. Dyn. Diff. Eqns. (2020).

[12] D. Gomez, L. Mei, J. Wei, *Hopf bifurcations from spike solutions for the weak coupling Gierer-Meinhardt system*, to appear, Europ. J. Appl. Math., (2020).

[13] D. Iron, M. J. Ward, J. Wei, *The stability of spike solutions to the one-dimensional Gierer-Meinhardt model*, Physica D, **150**(1-2), (2001), pp. 25–62.

[14] D. Iron, M. J. Ward, *The dynamics of multi-spike solutions for the one-dimensional Gierer-Meinhardt model*, SIAM J. Appl. Math., **62**(6), (2002), pp. 1924–1951.

[15] T. J. Kaper, T. Vo, *Delayed loss of stability due to the slow passage through Hopf bifurcations in reactiondiffusion equations*, Chaos 28, **091103** (2018).

[16] T. Kolokolnikov, F. Paquin-Lefebvre, M. J. Ward, *Stable Asymmetric Spike Equilibria for the Gierer-Meinhardt Model with a Precursor Field*, IMA J. Appl. Math., **85**(4), (2020), pp. 605–634.

[17] T. Kolokolnikov, M. J. Ward, J. Wei, *The existence and stability of spike equilibria in the one-dimensional Gray-Scott model: the pulse-splitting regime*, Physica D, **202**(3-4), (2005), pp. 258–293.

[18] T. Kolokolnikov, M. J. Ward, J. Wei, *The Existence and stability of spike equilibria in the one-dimensional Gray-Scott model: The low feed rate regime*, Studies in Appl. Math, **115**(1), (2005), pp. 21–71.

[19] P. Mandel, T. Erneux, *The slow passage through a steady bifurcation: delay and memory effects*, J. Stat. Phys., **48**(5-6), (1987), pp. 1059–1070.

[20] C. Muratov, V. V. Osipov, *Stability of the Static Spike Autosolitons in the Gray-Scott Model*, SIAM J. Appl. Math., **62**, No. 5, (2002), pp. 1463-1487.

[21] F. Paquin-Lefebvre, W. Nagata, M. J. Ward, *Weakly nonlinear theory for oscillatory dynamics in a 1-D PDE-ODE model of membrane dynamics coupled by a bulk diffusion field*, SIAM J. Appl. Math., **80**(3), (2020), pp. 1520–1545.

[22] W. Sun, M. J. Ward, R. Russell, *The slow dynamics of two-spike solutions for the Gray-Scott and Gierer-Meinhardt systems: competition and oscillatory instabilities*, SIAM J. App. Dyn. Sys., **4**(4), (2005), pp. 904–953.

[23] J. C. Tzou, Y. Nec, M. J. Ward, *The stability of localized spikes for the 1-D Brusselator reaction-diffusion model*, Europ. J. Appl. Math., **24**(4), (2013), pp. 515–564.

[24] J. C. Tzou, M. J. Ward, T. Kolokolnikov, *Slowly Varying Control Parameters, Delayed Bifurcations, and the Stability of Spikes in Reaction-Diffusion Systems*, Physica D, **290**(1), (2015), pp. 24–43.

[25] H. Van der Ploeg, A. Doelman, *Stability of spatially periodic pulse patterns in a class of singularly perturbed reaction-diffusion equations*, Indiana Univ. Math. J., **54**(5), (2005), pp. 1219–1301.

[26] F. Veerman, *Breathing pulses in singularly perturbed reaction-diffusion systems*, Nonlinearity, **28**, (2015), pp. 2211-2246.

[27] D. Walgraef, *Spatio-temporal pattern formation, with examples from physics, chemistry, and materials science, in book series, Partially ordered systems*, Springer, New York, (1997), 306 p.

[28] M. J. Ward, *Spots, traps, and patches: asymptotic analysis of localized solutions to some linear and nonlinear diffusive processes*, Nonlinearity, **31**(8), (2018), R189 (53 pages).

[29] M. J. Ward, J. Wei, *Hopf bifurcations and oscillatory instabilities of spike solutions for the one-dimensional Gierer-Meinhardt model*, J. Nonlinear Science, **13**(2), (2003), pp. 209-264.

[30] J. Wei, M. Winter, *Mathematical aspects of pattern formation in biological systems*, Applied Mathematical Science Series, Vol. 189, Springer, (2014).

[31] J. Wei, *Existence and stability of spikes for the Gierer-Meinhardt system*, book chapter in *Handbook of Differential Equations, Stationary Partial Differential Equations*, Vol. 5 (M. Chipot ed.), Elsevier, (2008), pp. 489–581.

[32] T. Wong, M. J. Ward, *Weakly nonlinear analysis of peanut-shaped deformations for localized spots of singularly perturbed reaction-diffusion systems*, SIAM J. Appl. Dyn. Sys., **19**(3), (2020), pp. 2030–2058.